Gastroenterology 2014;146:1048–1059

BASIC AND TRANSLATIONAL—LIVER

Vitamin D Receptor Activation Down-regulates the Small Heterodimer Partner and Increases CYP7A1 to Lower Cholesterol

Edwin C. Y. Chow,[1] Lilia Magomedova,[1] Holly P. Quach,[1,*] Rucha Patel,[1,*] Matthew R. Durk,[1] Jianghong Fan,[1] Han-Joo Maeng,[1] Kamdi Irondi,[1] Sayeepriyadarshini Anakk,[2] David D. Moore,[2] Carolyn L. Cummins,[1,§] and K. Sandy Pang[1,§]

[1]*Department of Pharmaceutical Sciences, Leslie Dan Faculty of Pharmacy, University of Toronto, Toronto, Ontario, Canada and* [2]*Department of Molecular and Cellular Biology, Baylor College of Medicine, Houston, Texas*

See editorial on page 899.

BACKGROUND & AIMS: Little is known about the effects of the vitamin D receptor (VDR) on hepatic activity of human cholesterol 7α-hydroxylase (CYP7A1) and cholesterol metabolism. We studied these processes in mice in vivo and mouse and human hepatocytes. **METHODS:** Farnesoid X receptor $(Fxr)^{-/-}$, small heterodimer partner $(Shp)^{-/-}$, and C57BL/6 (wild-type control) mice were fed normal or Western diets for 3 weeks and were then given intraperitoneal injections of vehicle (corn oil) or 1α,25-dihydroxyvitamin D_3 ($1,25[OH]_2D_3$; 4 doses, 2.5 μg/kg, every other day). Plasma and tissue samples were collected and levels of Vdr, Shp, Cyp7a1, Cyp24a1, and rodent fibroblast growth factor (Fgf) 15 expression, as well as levels of cholesterol, were measured. We studied the regulation of Shp by Vdr using reporter and mobility shift assays in transfected human embryonic kidney 293 cells, quantitative polymerase chain reaction with mouse tissues and mouse and human hepatocytes, and chromatin immunoprecipitation assays with mouse liver. **RESULTS:** We first confirmed the presence of Vdr mRNA and protein expression in livers of mice. In mice fed normal diets and given injections of $1,25(OH)_2D_3$, liver and plasma concentrations of $1,25(OH)_2D_3$ increased and decreased in unison. Changes in hepatic *Cyp7a1* messenger RNA (mRNA) correlated with those of *Cyp24a1* (a Vdr target gene) and inversely with *Shp* mRNA, but not ileal *Fgf15* mRNA. Similarly, incubation with $1,25(OH)_2D_3$ increased levels of *Cyp24a1/CYP24A1* and *Cyp7a1/CYP7A1* mRNA in mouse and human hepatocytes, and reduced levels of *Shp* mRNA in mouse hepatocytes. In $Fxr^{-/-}$ and wild-type mice with hypercholesterolemia, injection of $1,25(OH)_2D_3$ consistently reduced levels of plasma and liver cholesterol and *Shp* mRNA, and increased hepatic *Cyp7a1* mRNA and protein; these changes were not observed in $Shp^{-/-}$ mice given $1,25(OH)_2D_3$ and fed Western diets. Truncation of the human small heterodimer partner (SHP) promoter and deletion analyses revealed VDR-dependent inhibition of *SHP*, and mobility shift assays showed direct binding of VDR to enhancer regions of *SHP*. In addition, chromatin immunoprecipitation analysis of livers from mice showed that injection of $1,25(OH)_2D_3$ increased recruitment of Vdr and rodent retinoid X receptor to the *Shp* promoter. **CONCLUSIONS:** Activation of the VDR represses hepatic SHP to increase levels of mouse and human CYP7A1 and reduce cholesterol.

Keywords: Liver; Bile Acid; Farnesoid X Receptor; Transcriptional Regulation.

Cholesterol is an essential component of cell membranes and the precursor to steroid hormones and bile acids. In excess, cholesterol can lead to atherosclerosis and coronary heart disease. In liver, cholesterol is metabolized to bile acids by cholesterol 7α-hydroxylase (CYP7A1), which is the rate-limiting metabolic enzyme in the classic bile acid synthetic pathway.[1] The *CYP7A1* promoter contains highly conserved bile acid responsive regions known to be modulated by feedback repression by various transcription factors in response to increasing hepatic bile acid concentrations.[1] A primary, negative feedback mechanism of CYP7A1 regulation is the human farnesoid X receptor ([FXR] NR1H4) and human small heterodimer partner ([SHP] NR0B2) regulatory cascade.[2] Bile acids such as chenodeoxycholic acid (CDCA) activate FXR to increase transcription of SHP, an atypical nuclear receptor that lacks a DNA binding domain and represses CYP7A1 activation by suppression of transcription factors, liver receptor homolog-1 (NR5A2) and hepatocyte nuclear factor 4α (NR2A1), which are essential for CYP7A1 expression.[3] A second negative feedback mechanism on CYP7A1 is found in the intestine, where activation of FXR induces fibroblast growth factor 15/19 (rodent/human), a hormonal signaling molecule that represses CYP7A1 through interaction with the liver fibroblast growth factor receptor 4 via the *c*-Jun signaling pathway.[4]

*Authors share co-third authorship; §Authors share co-senior authorship.

Abbreviations used in this paper: **Asbt, rodent apical sodium dependent bile acid transporter; CDCA, chenodeoxycholic acid; ChIP, chromatin immunoprecipitation; Cyp7a1/CYP7A1, rodent/human cholesterol 7α-hydroxylase; $1,25[OH]_2D_3$, 1α,25-dihydroxyvitamin D_3; EMSA, electromobility shift assays; Fgf15, rodent fibroblast growth factor 15; Fxr/FXR, rodent/human farnesoid X receptor; HDL-C, high-density lipoprotein cholesterol; HMGCo-A, human 3-hydroxy-3-methyl-glutaryl-CoA; LDL-C, low-density lipoprotein cholesterol; Lrh-1, rodent liver receptor homolog 1; mRNA, messenger RNA; Rxrα, rodent retinoid X receptor-α; Shp/SHP, rodent/human small heterodimer partner; VDRE, vitamin D receptor response element.**

© 2014 by the AGA Institute
0016-5085/$36.00
http://dx.doi.org/10.1053/j.gastro.2013.12.027

The vitamin D receptor ([VDR] NR1I1) binds to its endogenous ligand, 1α,25-dihydroxyvitamin D_3 (1,25 $[OH]_2D_3$) or lithocholic acid (alternate VDR ligand)[5] to activate the transcription of genes. Various mechanisms implicate a role for VDR on CYP7A1 regulation.[6] Activation of VDR was found to antagonize the CDCA-dependent transactivation of FXR in VDR-transfected HepG2 cells[7] and blunt the Lxrα-mediated induction of Cyp7a1 mRNA in rat hepatoma cells.[8] VDR inhibition of CYP7A1 transcription in human hepatocytes and HepG2 cells has been attributed to blockage of hepatocyte nuclear factor 4α−mediated activation of CYP7A1.[9] Induction of intestinal Fgf15 after a high dose of $1,25(OH)_2D_3$ in mice was shown to down-regulate Cyp7a1 messenger RNA (mRNA) level.[10] By contrast, *Vdr*-knockout mice are reported to have higher total serum cholesterol,[11] and treatment with 1α-hydroxyvitamin D_3, a potent $1,25(OH)_2D_3$ precursor, up-regulated Cyp7a1 mRNA expression in mice.[12,13] Likewise, doxercalciferol, a vitamin D analogue, decreased the accumulation of triglycerides and cholesterol in murine kidney.[14] In rat, $1,25(OH)_2D_3$ down-regulated liver Cyp7a1 by an indirect mechanism.[15] The divergent views are partially reconciled by species differences, with VDR protein levels being extremely low in rat liver, but present at detectable levels in mouse and man.[16] The down-regulation of Cyp7a1 after $1,25(OH)_2D_3$ treatment in the rat is explained as a secondary hepatic Fxr and not Vdr effect, because increased bile acid absorption into portal blood occurred as a result of Vdr-mediated induction of the intestinal apical sodium-dependent bile acid transporter (Asbt).[15] Clinical reports relating vitamin D status to cholesterol (cholesterol levels vs $1,25[OH]_2D_3$ or its less active precursor, 25-hydroxyvitamin D_3, $25[OH]D_3$) are equivocal. Both short-term[17] and long-term[18] vitamin D treatment did not improve lipid profiles or lower cholesterol and only resulted in slightly lower serum triglyceride, while other studies documented increased high-density lipoprotein cholesterol (HDL-C),[19] or decreased total cholesterol and triglyceride but unchanged HDL-C and low-density lipoprotein cholesterol (LDL-C) levels.[20] A recent, population-based study established an association between $1,25(OH)_2D_3$ and HDL-C and $25(OH)D_3$ and total cholesterol, LDL-C, and triglyceride.[21] Atorvastatin,

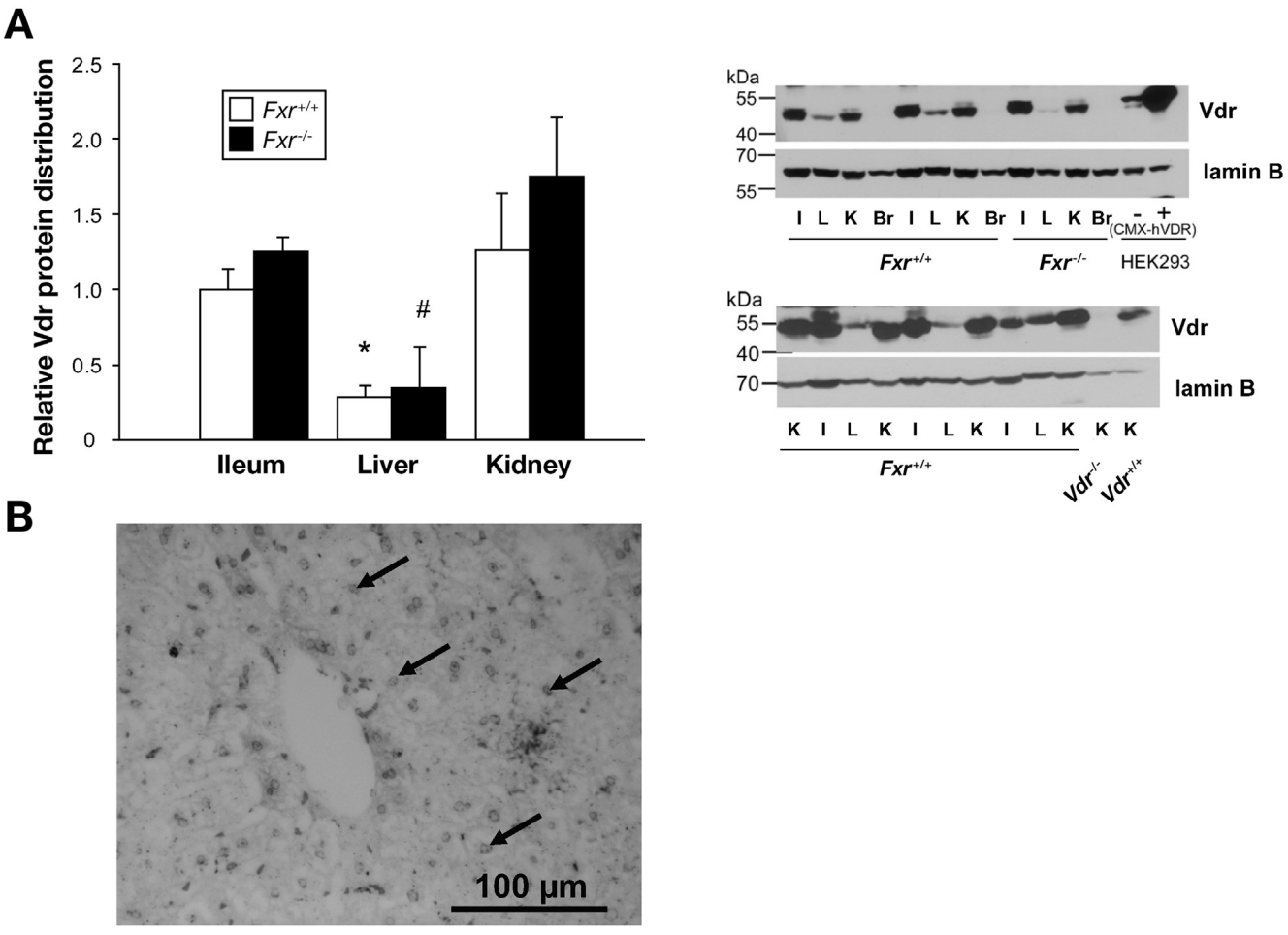

Figure 1. Vdr protein distribution in mouse and liver immunostaining. (*A*) Nuclear Vdr protein expression in 50 μg ileum (I), liver (L), kidney (K), and brain (Br) of wild-type and $Fxr^{-/-}$ mice, with human embryonic kidney 293 cells transfected with CMX (basal levels) (−) or overexpressing CMX-Vdr (+) as standards (*top panel*), vs kidney samples of $Vdr^{-/-}$ and $Vdr^{+/+}$ mice (*lower panel*). Vdr protein expression was similar between $Fxr^{+/+}$ and $Fxr^{-/-}$ livers (approximately 30% of I or K), but absent in $Vdr^{-/-}$ kidney ($n = 3–4$); $^{*,\#}P < .05$ vs ileum for $Fxr^{+/+}$ and $Fxr^{-/-}$ mice, respectively (Mann-Whitney *U* test). (*B*) Vdr protein (*arrows*) was present within nuclei of hepatocytes of wild-type mice.

supplemented with vitamin D, further lowered total cholesterol and LDL-C,[22] and patients receiving statin or niacin supplemented with vitamin D and fish oil showed reduced LDL-C and triglycerides and elevated HDL-C.[23] The role of the VDR in liver cholesterol regulation remains controversial.

The intent of this study was to clarify the impact of Vdr on Cyp7a1 regulation and cholesterol lowering. We verified the

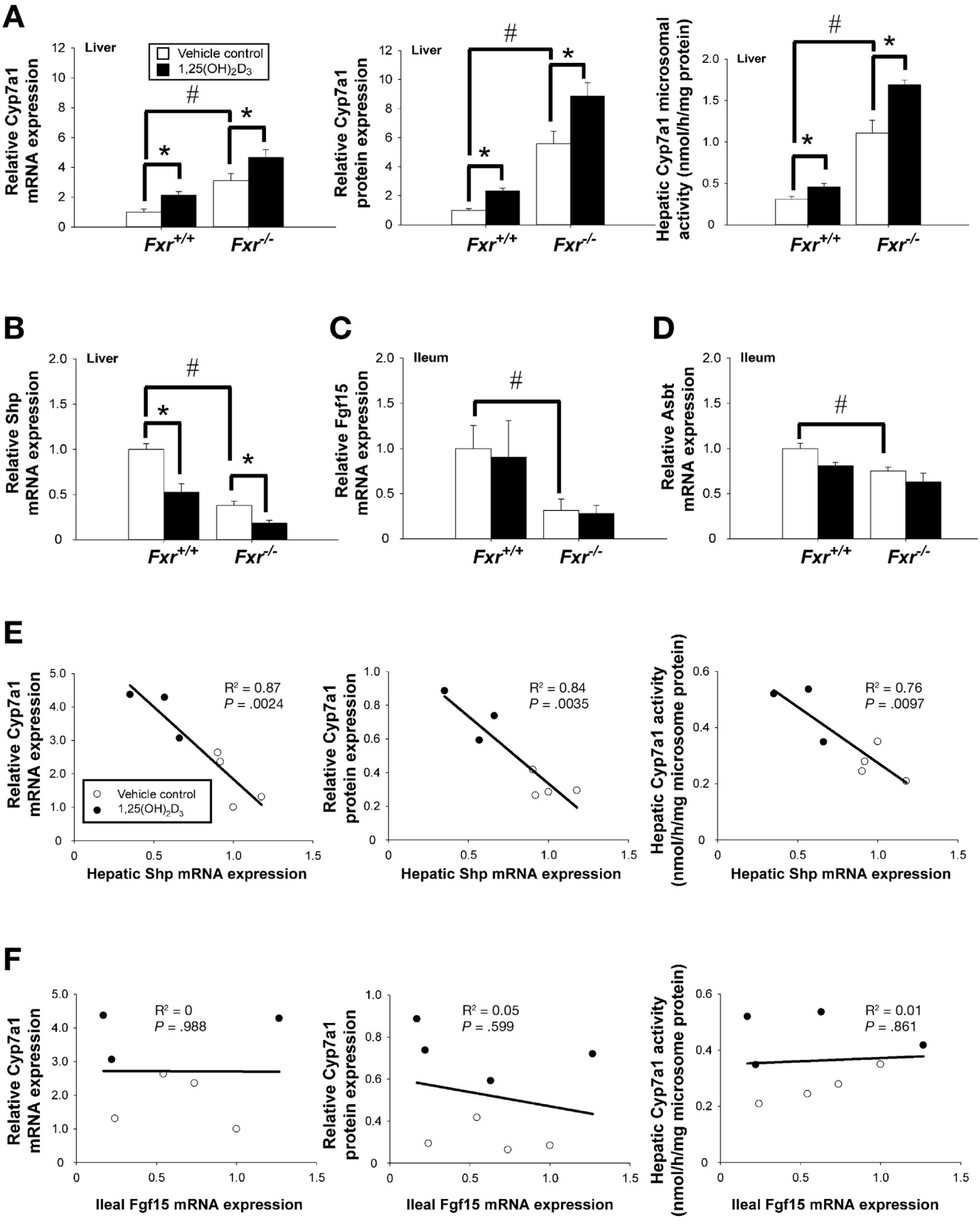

presence of Vdr in murine liver, and demonstrated that $1,25(OH)_2D_3$ given to mice rapidly reached the liver, resulting in induction of hepatic Cyp7a1 via down-regulation of rodent small heterodimer partner (Shp). We showed that Vdr-mediated Shp repression and up-regulation of Cyp7a1 was Fxr independent but Shp dependent in vivo. Luciferase reporter, electrophoretic mobility shift assay (EMSA), and chromatin immunoprecipitation (ChIP) assays further supported a direct role for Vdr/VDR in the repression of Shp/SHP to result in up-regulation of *Cyp7a1/CYP7A1*, providing a novel mechanism for cholesterol lowering. In mouse and human hepatocytes, Cyp7a1/CYP7A1 expression was elevated on exposure to $1,25(OH)_2D_3$.

Materials and Methods

In the Supplementary Material, we provide information on materials, mouse strains, antibodies, plasmids, and procedures for real-time polymerase chain reaction, Western blotting, microsomal preparation for Cyp7a1 activity, and assay procedures for bile acid pool size, cholesterol, and $1,25(OH)_2D_3$.

Immunostaining of Murine Liver Vdr

Livers of male C57BL/6 mice were perfusion-fixed with phosphate-buffered saline and 4% paraformaldehyde, and kept overnight at 4°C. Then, 7-μm-thick paraffin-embedded sections were dewaxed and incubated in 2N HCl at 37°C for 30 minutes. Sections were preblocked with 5% goat serum in phosphate-buffered saline containing 0.1% Tween-20, then incubated with the primary anti-VDR antibody 9A7 (1:50 v/v) overnight. After rinsing 3 times with 5% goat serum in phosphate-buffered saline containing 0.1% Tween-20, the secondary goat anti-rat horseradish peroxidase antibody was added for 2 hours at room temperature and visualized using a metal-enhanced 3,3′-diaminobenzidine tetrahydrochloride substrate kit (Thermo Scientific, Rockford, IL). After several washes, sections were imaged using a Nikon E1000R microscope.

$1,25(OH)_2D_3$ Treatment of Mice in vivo

In each set of in vivo studies, doses of 0 or 2.5 μg/kg $1,25(OH)_2D_3$, in sterile corn oil were given intraperitoneally every other day for 8 days at 9 to 10 AM.[24] First, we treated normal-diet–fed, male C57BL/6 (wild-type or $Fxr^{+/+}$] and $Fxr^{-/-}$ mice (8 to 12 weeks; n = 4–10) with $1,25(OH)_2D_3$, and blood and tissues were harvested on day 8 between 12 PM and 2 PM. In the second study, blood samples and livers from wild-type mice were collected at different time points during the $1,25(OH)_2D_3$ treatment period, as described.[25] In the third study, hypercholesterolemic models composed of wild-type, $Fxr^{-/-}$, and $Shp^{-/-}$ mice (6–8 weeks old; n = 4–10) fed a Western diet (Harlan Teklad Cat #88137; high-fat [42%]/high-cholesterol [0.2%] diet) for 3 weeks were established, a period during which Cyp7a1 mRNA/protein expression was unchanged. These mice were given 4 repeated doses of $1,25(OH)_2D_3$ every other day at the beginning of the third week of the Western diet. On day 8, systemic and portal blood samples and tissues were obtained under anesthesia, as previously described.[15,24] Basal mRNA levels of intestinal and liver genes in $Fxr^{-/-}$ and $Shp^{-/-}$ mice were compared with those of wild-type mice (Supplementary Figure 1*A* and *B*). $1,25(OH)_2D_3$ treatment resulted in a slight elevation of plasma calcium, but relatively unchanged phosphorous, alanine aminotransferase, and portal bile acid levels (Supplementary Table 1).

Mouse Primary Hepatocytes

Mouse primary hepatocytes were isolated[26] and treated with vehicle (0.1% EtOH) or 100 nM $1,25(OH)_2D_3$ (M199 media without fetal bovine serum) for 0, 3, 6, 9, 12, and 24 hours. Cells were harvested for mRNA determination at 9 hours, the minimal time required for induction of Cyp24a1.[27] Dose-dependent activation of Cyp24a1 by $1,25(OH)_2D_3$ (10 to 250 nM) was observed (data not shown).

Human Hepatocytes

Upon arrival, the cold preservation medium for storage of human primary hepatocytes (gift from Dr Jasminder Sahi, Life Technologies, TX) was replaced with Williams E medium (Cat# CM4000, Life Technologies, TX), supplemented with the cell maintenance cocktail (10 mM of dexamethasone, 120 U/mL penicillin, and 120 U/mL streptomycin, 2 mM GlutaMax, 15 mM of HEPES and ITS+ 6.25 g/mL insulin, 6.25 g/mL transferrin, 6.25 g/mL selenous acid, 1.25 mg/mL bovine serum albumin, and 5.33 g/mL linoleic acid were used in dilutions according to manufacture's instructions). Plates (24-wells; 2.1×10^6 cells/cm^2) were acclimatized overnight at 37°C in a humidified incubator. On the next day, cells were treated with vehicle (0.1% ethanol) or 100 nM $1,25(OH)_2D_3$ and harvested at 3, 6, 12, and 24 hours. Activation of VDR was confirmed by CYP24A1 mRNA induction.

Transfection Assays of Human Embryonic Kidney 293 Cells

Cell transfection was performed in media containing 10% charcoal-stripped fetal bovine serum using calcium phosphate in 96-well plates. The total amount of plasmid DNA (150 ng/well) included 50 ng reporter, 20 ng pCMX-β-galactosidase, 15 ng nuclear receptor, 15 ng pCMX-liver receptor homolog 1 (Lrh-1), and pGEM filler plasmid. Ligands were added at 6 to 8 hours post transfection. Cells harvested 14 to 16 hours later were assayed for luciferase and β-galactosidase activity.

Figure 2. $1,25(OH)_2D_3$ treatment increases Cyp7a1 mRNA, protein, and microsomal activity and decreases hepatic Shp expression in normal-diet–fed wild-type and $Fxr^{-/-}$ mice. (*A*) Cyp7a1 mRNA, protein (normalized to rodent glyceraldehyde-3-phosphate dehydrogenase), and microsomal activity were increased after $1,25(OH)_2D_3$ treatment in both wild-type and $Fxr^{-/-}$ mice. (*B*) Hepatic Shp mRNA was decreased, and ileal (*C*) Fgf15 and (*D*) Asbt mRNA were unchanged (n = 4–10); $^{\#}P < .05$ between $Fxr^{-/-}$ vs wild-type vehicle-treated mice; $^{*}P < .05$ between vehicle vs treated mice of the same genotype (Mann-Whitney *U* test). A significant, negative correlation (each point represents one mouse) exists between (*E*) Cyp7a1 mRNA/protein/activity and liver Shp (*F*), but not ileal Fgf15 mRNA in wild-type mice (n = 3–4).

Luciferase values were normalized to β-galactosidase to control for transfection efficiency and expressed as relative luciferase units.

Nuclear Protein Extracts

Human embryonic kidney 293 cells were transfected with 10 μg Vdr, rodent retinoid X receptor-α (Rxrα), or CMX plasmid DNA using calcium phosphate in 10-cm plates. At 30 hours post transfection, nuclear protein extracts were prepared.[26]

Electrophoretic Mobility Shift Assay

Oligonucleotide sequences are described in Supplementary Table 2. Oligos were biotinylated using a biotin 3′ end DNA labeling kit (Pierce, Rockford, IL). DNA binding reactions consisted of 2.5 μL of NE-PER nuclear extracts in binding buffer (10 mM Tris, 50 mM KCl, 1 mM dithiothreitol, 1 mM EDTA, 5% glycerol, 1 μg BSA and 1 μg poly(dI-dC); [pH 7.5]). After a 20-minute preincubation, 50 fmol annealed biotinylated DNA was added and incubated for 30 minutes on ice. Reactions were loaded onto a 6% polyacrylamide gel, transferred to Biodyne B membrane (Pierce) and cross-linked. Detection was carried out using the Light Shift Chemiluminescent EMSA Kit (Pierce).

ChIP

ChIP assays were performed on frozen livers after vehicle or $1,25(OH)_2D_3$ treatment in normal-diet–fed wild-type mice (3–4 sets of experiment, in triplicate) at 12 hours after the fourth injection, as described.[26] Liver nuclei were resuspended in 2× pellet volume of sonication buffer (0.2% sodium dodecyl sulfate, 1% Triton-X, 0.1% Na-deoxycholate, 1 mM EDTA and 50 mM Tris-HCl [pH 8.0], 150 mM NaCl, and protease inhibitors). Chromatin, diluted 2-fold in buffer (sonication buffer without sodium dodecyl sulfate) and 400 μL diluted sample, were incubated with 10 μg Vdr, Rxrα, Lrh-1, or 2 μg H3K9me3 antibodies (see Supplementary Material) overnight and used for immunoprecipitation. After spin column purification, the eluate was diluted 5-fold with water, and quantitative polymerase chain reaction was performed using 5 μL template DNA with the

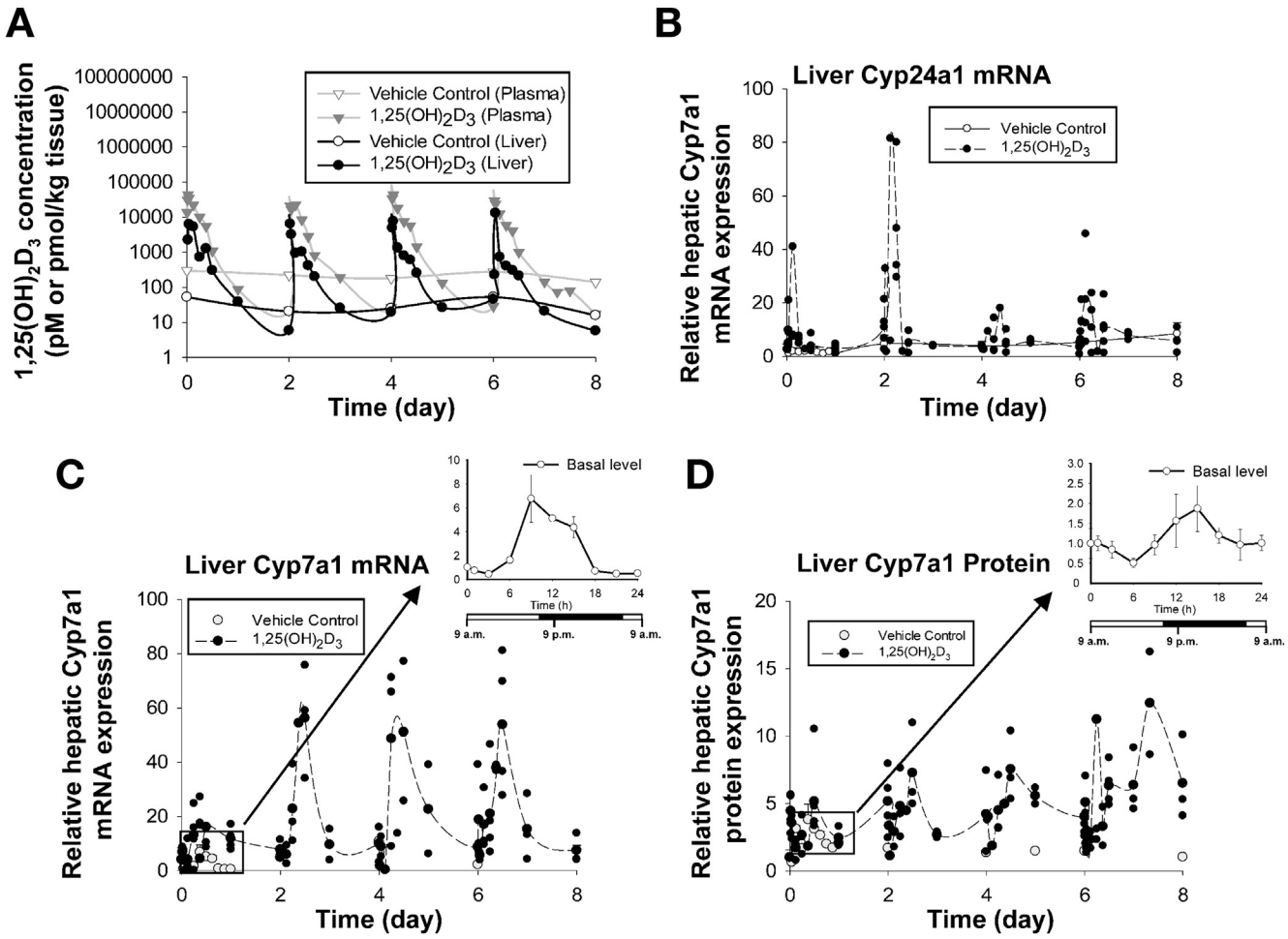

Figure 3. Correlation between liver $1,25(OH)_2D_3$ concentration and hepatic Cyp24a1 and Cyp7a1 mRNA expression in normal-diet–fed wild-type mice. Repeated administration of $1,25(OH)_2D_3$ resulted in (*A*) biphasic decay of $1,25(OH)_2D_3$ concentration in liver (mean points; n = 2–4; *solid* and *open circles* for levels in treated livers or basal levels in vehicle-treated livers) that paralleled those in plasma (*gray solid* and *open symbols* for treated and basal levels in vehicle-treated livers; previously published[25]) and corresponding changes in hepatic (*B*) Cyp24a1 mRNA, (*C*) Cyp7a1 mRNA, (*D*) Cyp7a1 protein expression (n = 2–4). The insets show the diurnal variation of basal Cyp7a1 mRNA and protein expression, peaking at around 9 PM and 12 AM, respectively, in vehicle-treated mice. For (*B*) to (*D*), each point represents datum from one mouse, except for insets in (*C*) and (*D*), where the open symbols denote mean values (n = 2–4).

following primer set: forward: 5′-GAGCGCCTGAGACCTTGGT-3′ and reverse: 5′-TCAAGTGCATAAACAGGGTCATTAA-3′ amplifying the putative mouse Shp VDRE. Quantification was performed by quantitative polymerase chain reaction (standard curve method) using serial dilutions of the input as standards.

Statistics

Data are expressed as mean ± SEM for in vivo data and mean ± SD for in vitro data. For comparison of in vivo and in vitro data between 2 groups, the Mann-Whitney *U* test and the unpaired Student *t* tests were used, respectively, and $P < .05$ was set as the level of significance.

Results

Vdr Protein Tissue Distribution and Liver Immunostaining

Nuclear Vdr protein was present at similar levels in the ileum and kidney of wild-type and $Fxr^{-/-}$ mice, although levels were considerably lower in liver and brain, as found previously.[24,25] Vdr protein was found in the lysate of primary hepatocytes prepared from wild-type mice (data not shown) and $Vdr^{+/+}$ but not $Vdr^{-/-}$ kidney (Figure 1*A*). Vdr protein was identified in mouse hepatocytes by immunostaining (Figure 1*B*), and specificity of the antibody was further confirmed by staining liver sections or Western blots of livers obtained from $Vdr^{-/-}$ mice (data not shown).

$1,25(OH)_2D_3$ Increases Hepatic Cyp7a1 and Decreases Hepatic Shp But Not Ileal Fgf15 in Normal-Diet–Fed $Fxr^{+/+}$ and $Fxr^{-/-}$ Mice

The $Fxr^{-/-}$ mouse was used to circumvent potential confounding effects of feedback regulation of cholesterol metabolism through hepatic Fxr.[15] Absence of Fxr in $Fxr^{-/-}$ mice resulted in higher basal hepatic Cyp7a1 mRNA, protein, and microsomal activity (Figure 2*A*) compared to those of $Fxr^{+/+}$ mouse, and lower mRNA basal levels of hepatic Shp and intestinal Fgf15 and Asbt (Figure 2*B*–*D*). Remarkably, $1,25(OH)_2D_3$ treatment resulted in significant up-regulation of hepatic Cyp7a1 mRNA and protein expression and microsomal activity in both $Fxr^{+/+}$ and $Fxr^{-/-}$ genotypes (Figure 2*A*), accompanied by a reduction in hepatic Shp mRNA expression without changes in intestinal Fgf15 and Asbt (Figures 2*B*–*D*). There was a significant, negative correlation between Cyp7a1 mRNA/protein/microsomal

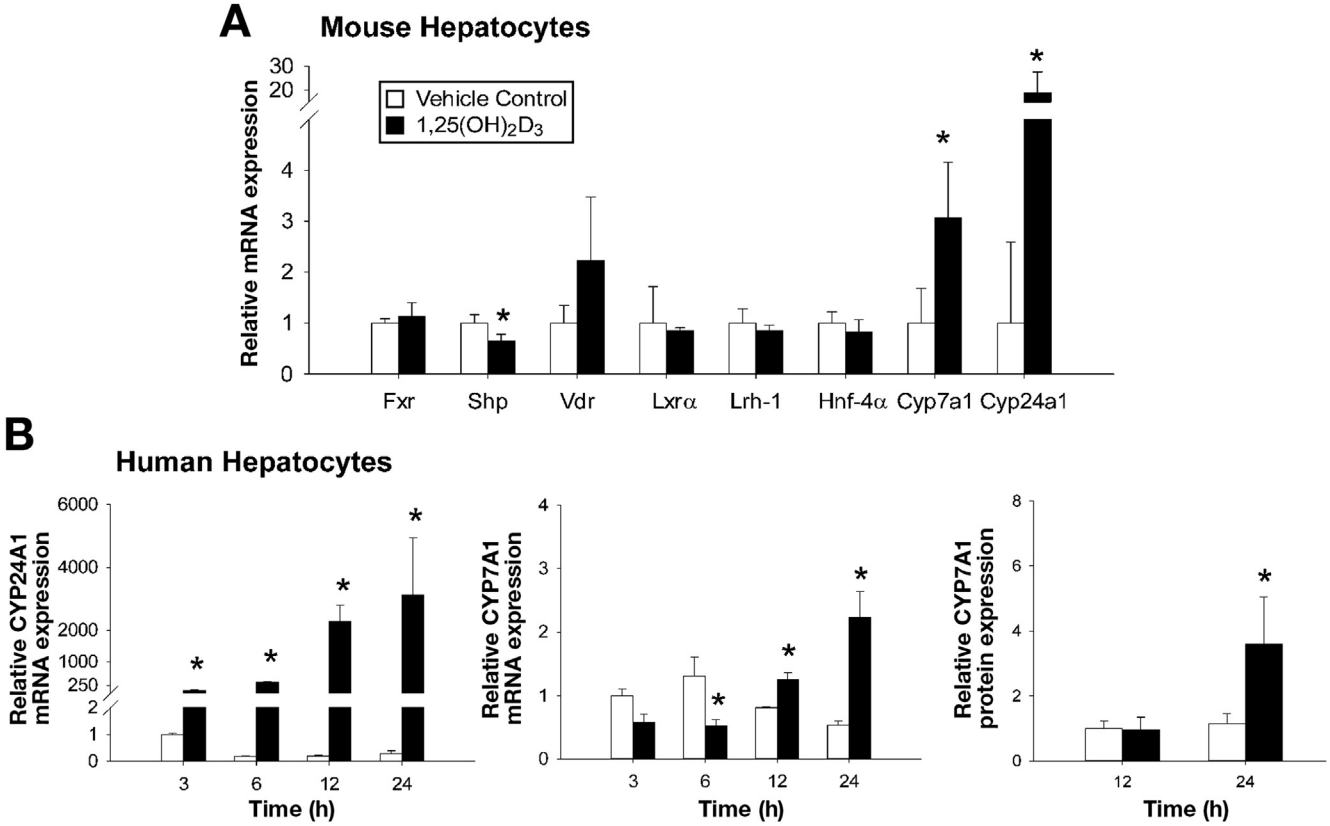

Figure 4. $1,25(OH)_2D_3$ treatment changes Cyp24a1/CYP24A1 and Cyp7a1/CYP7A1, and Shp mRNA expression in wild-type mouse and human primary hepatocytes. (*A*) Freshly isolated mouse hepatocytes showed increased Cyp7a1 and Cyp24a1 and reduced Shp mRNA expression at 9 hours after 100 nM $1,25(OH)_2D_3$ treatment and (*B*) human hepatocytes (from the same donor) exposed to 100 nM $1,25(OH)_2D_3$ vs vehicle showed time-dependent induction of CYP24A1 and CYP7A1 mRNA and CYP7A1 protein. Data are from 1 donor and presented as mean ± SD (n = 3) of triplicates. $P < .05$: *compared with vehicle control (*t* test).

activity and hepatic Shp (Figure 2*E*), but not intestinal Fgf15 mRNA expression (Figure 2*F*), suggesting that attenuation of Shp resulted in elevated Cyp7a1, independent of Fxr.

Parallel Changes in Liver 1,25(OH)$_2$D$_3$ Concentrations and Temporal Cyp7a1 and Cyp24a1 mRNA Expression in Wild-Type Mice

To further examine Cyp7a1 expression changes in response to Vdr activation, we systematically analyzed the relationship between liver 1,25(OH)$_2$D$_3$ concentration and gene expression in normal-diet–fed wild-type mice throughout the 1,25(OH)$_2$D$_3$ treatment period. A diurnal variation was found in both basal Cyp7a1 mRNA and protein levels (*insets* of Figure 3*C* and *D*), with peaks occurring at around 9 PM and 12 AM, respectively. After 1,25(OH)$_2$D$_3$ dosing, a biphasic decay profile of liver 1,25(OH)$_2$D$_3$ that closely paralleled the plasma concentration-time curve[25] was observed (Figure 3*A*). In response to increased liver 1,25(OH)$_2$D$_3$, hepatic Cyp24a1 mRNA levels rose, occurring maximally between 3 and 6 hours post injection (Figure 3*B*). Cyp7a1 mRNA expression also rose maximally at around 12 hours post injection, and levels were amplified with subsequent injections (60 and 80-fold higher; Figure 3*C*). Patterns of Cyp7a1 mRNA and protein induction were similar (Figures 3C and 3D). The increase in Cyp7a1 mRNA expression in response to 1,25(OH)$_2$D$_3$ was much higher (60- to 80-fold) than the peak of the circadian rhythm (6.7-fold, Figure 3*C*).

1,25(OH)$_2$D$_3$ Increases Cyp7a1/CYP7A1 and Cyp24a1/CYP24A1 mRNA Levels in Mouse and Human Primary Hepatocytes

To confirm that changes in Cyp7a1 and Shp mRNA were independent of other physiologic signaling molecules from the gut or portal circulation, isolated mouse primary hepatocytes were incubated with 100 nM 1,25(OH)$_2$D$_3$. A significant decrease in Shp (35%) with subsequent increase in Cyp7a1 (3-fold) and Cyp24a1 (19-fold) mRNA expression was observed at 9 hours (Figure 4*A*), confirming an autonomous role for 1,25(OH)$_2$D$_3$ in the modulation of Cyp7a1 via SHP repression in hepatocytes. Human primary hepatocytes exposed to 100 nM 1,25(OH)$_2$D$_3$ showed increased human CYP24A1 and CYP7A1 mRNA expression at 12 and 24 hours,

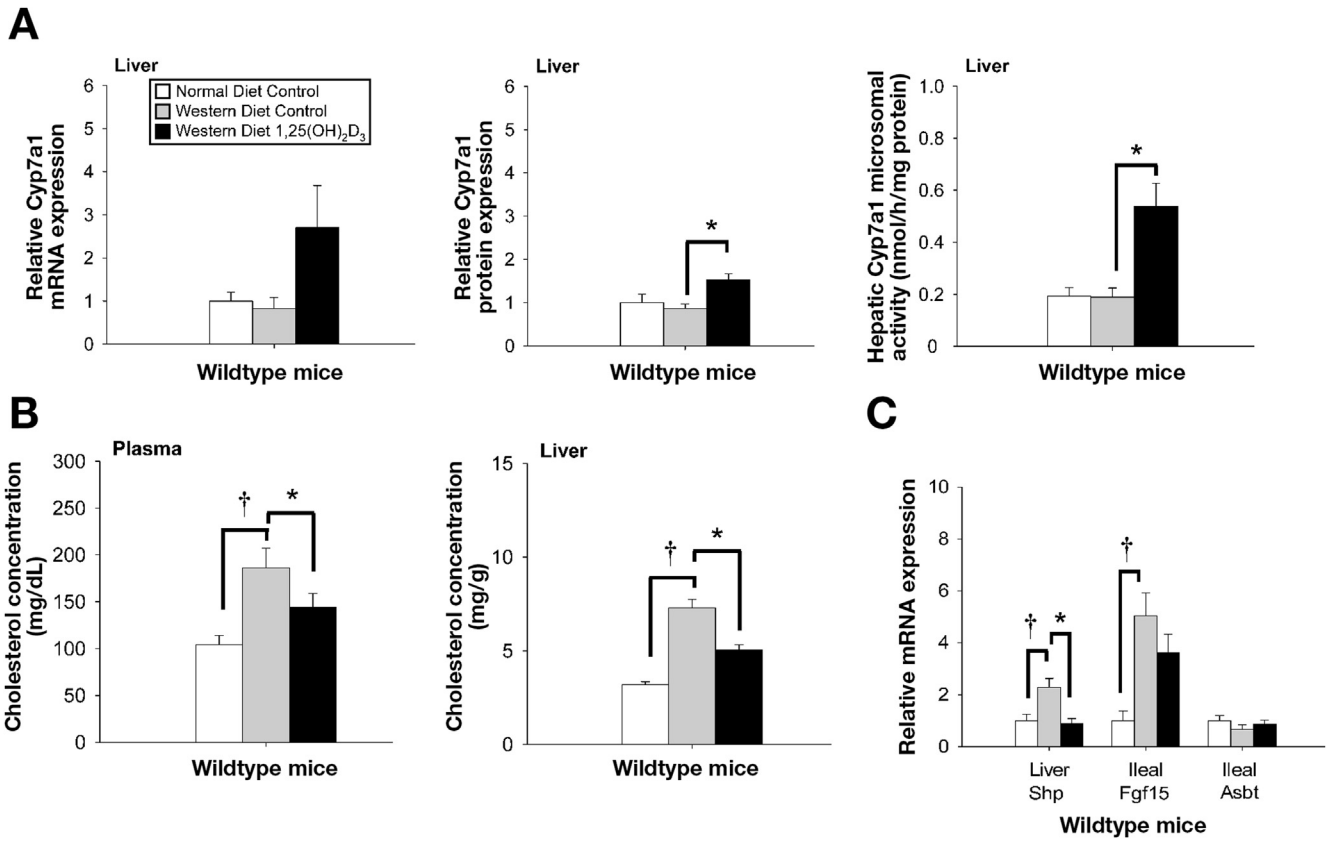

Figure 5. 1,25(OH)$_2$D$_3$ treatment increases hepatic Cyp7a1 and decreases hepatic Shp mRNA expression and plasma and liver cholesterol in Western-diet–fed, wild-type mice. (*A*) Hepatic Cyp7a1 protein and microsomal activity were increased after 1,25(OH)$_2$D$_3$ treatment. (*B*) Plasma and liver cholesterol concentrations, elevated with the Western diet, were reduced after 1,25(OH)$_2$D$_3$ treatment compared with Western-diet–fed controls. (*C*) Hepatic Shp mRNA expression was increased with Western diet, which decreased with 1,25(OH)$_2$D$_3$ treatment. The Western diet increased ileal Fgf15 mRNA level, which remained relatively unchanged with 1,25(OH)$_2$D$_3$ treatment (n = 4–8); $P < .05$: †Western diet vs normal diet; *Western-diet–fed, vehicle-treated control vs Western-diet–fed, 1,25(OH)$_2$D$_3$-treated mice (Mann-Whitney *U* test).

respectively, and CYP7A1 protein expression at 24 hours (Figure 4*B*). Hepatocytes from 2 other human donors displayed similar trends (data not shown).

In Hypercholesterolemic Wild-Type Mice, 1,25(OH)$_2$D$_3$ Increases Hepatic Cyp7a1 and Lowers Cholesterol by Decreasing Hepatic Shp Without Changing Ileal Fgf15

The Western diet did not alter Cyp7a1 expression or microsomal activity of wild-type mice (Figure 5*A*), but increased plasma and liver cholesterol levels (Figure 5*B*) and hepatic Shp and ileal Fgf15 mRNA expression (Figure 5*C*). The 1,25(OH)$_2$D$_3$ treatment increased Cyp7a1 protein expression (76%) and microsomal activity (280%) (Figure 5*A*) and lowered both plasma and liver cholesterol (Figure 5*B*) and hepatic Shp mRNA expression (Figure 5*C*). The bile acid pool size and fecal bile acid excretion were significantly increased after 1,25(OH)$_2$D$_3$ treatment (Supplementary Figure 1*C*), suggesting that increased Cyp7a1 activity led to more bile acid formation. There was, however, little change in the portal bile acid concentration (Supplementary Table 1) and absence of significant change in other cholesterol-related genes in the intestine and liver (Supplementary Figure 2).

In Hypercholesterolemic Fxr$^{-/-}$ and Shp$^{-/-}$ Mouse Models, 1,25(OH)$_2$D$_3$ Reduced Plasma and Liver Cholesterol in Fxr$^{-/-}$ Mice But Not Shp$^{-/-}$ Mice

To examine whether Fxr and Shp are involved in cholesterol lowering, we fed *Fxr*$^{-/-}$ and *Shp*$^{-/-}$ mice with the same Western diet and used the same 1,25(OH)$_2$D$_3$ injection regimen as that for wild-type mice. Western diet alone did not alter basal Cyp7a1 levels (Figure 6*A* and *D*), but increased plasma and liver cholesterol concentrations in Western-diet–fed *Fxr*$^{-/-}$ (Figure 6*B*), although not Western-diet–fed *Shp*$^{-/-}$ mice (Figure 6*E*). Basal hepatic Shp mRNA level was higher, and ileal Asbt mRNA level, slightly lower, in Western-diet–fed compared with normal-diet–fed *Fxr*$^{-/-}$ controls (Figure 6*C*), and basal ileal Fgf15 mRNA expression was higher in both Western-diet–fed *Fxr*$^{-/-}$ and *Shp*$^{-/-}$ controls (Figures 6*C* and *F*).

The 1,25(OH)$_2$D$_3$ treatment increased Cyp7a1 mRNA and protein expression in *Fxr*$^{-/-}$ (Figure 6*A*), but not in

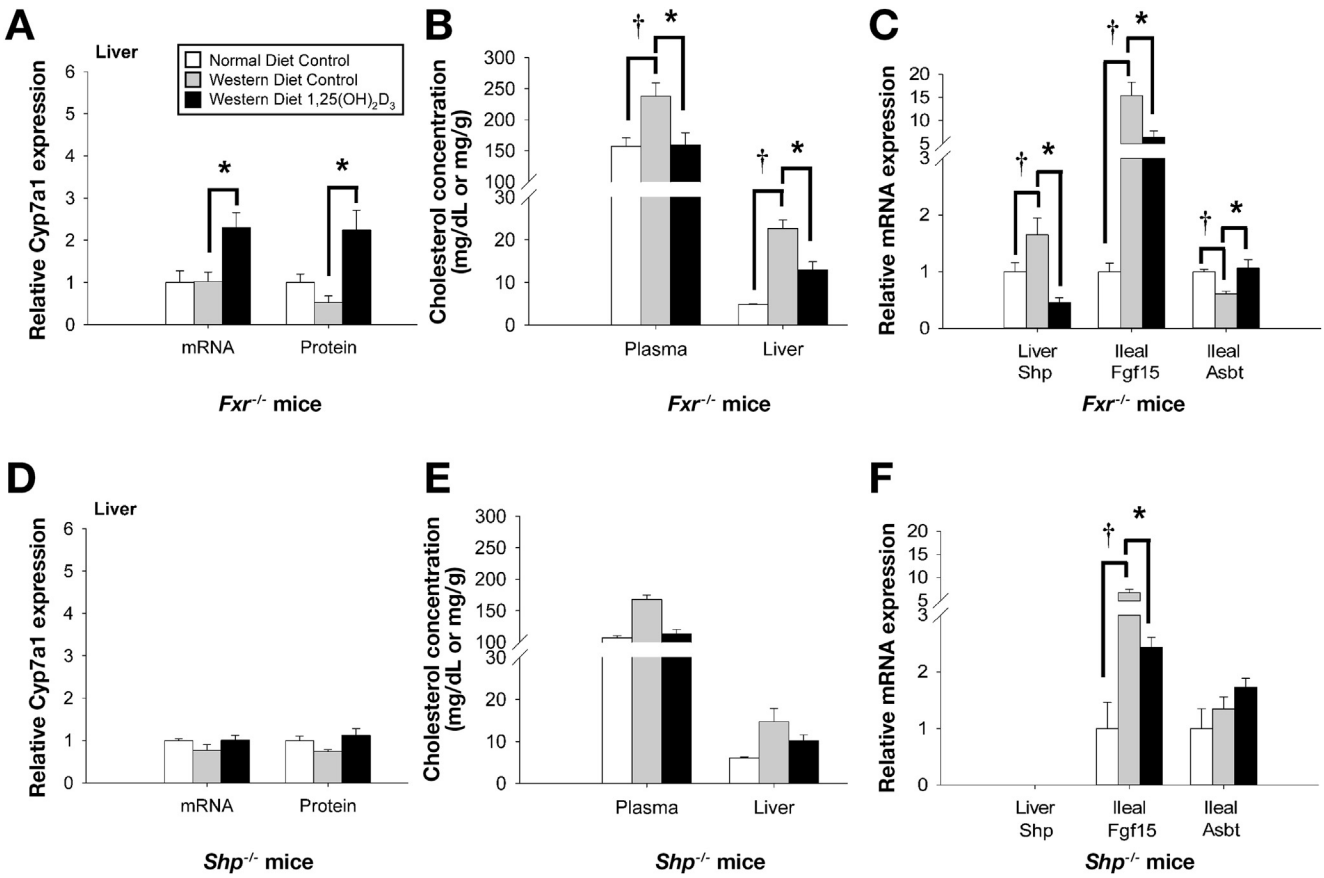

Figure 6. 1,25(OH)$_2$D$_3$ treatment lowers plasma and liver cholesterol in Western-diet–fed *Fxr*$^{-/-}$ but not *Shp*$^{-/-}$ mice. 1,25(OH)$_2$D$_3$-treatment (*A*) increased Cyp7a1 mRNA and protein expression, (*B*) decreased plasma and liver cholesterol concentrations, and (*C*) attenuated hepatic Shp, ileal Fgf15, and increased ileal Asbt mRNA levels in Western-diet–fed *Fxr*$^{-/-}$ mice; and Cyp7a1 expression and cholesterol levels [(*D*) to (*E*)] were unchanged in 1,25(OH)$_2$D$_3$-treated Western-diet–fed *Shp*$^{-/-}$ mice, although ileal Fgf15 mRNA expression was decreased (n = 4–8) (*F*); $P < .05$: †Western diet vs normal diet; *vehicle-treated, Western-diet–fed control vs Western-diet–fed, 1,25(OH)$_2$D$_3$-treated mice (Mann-Whitney *U* test).

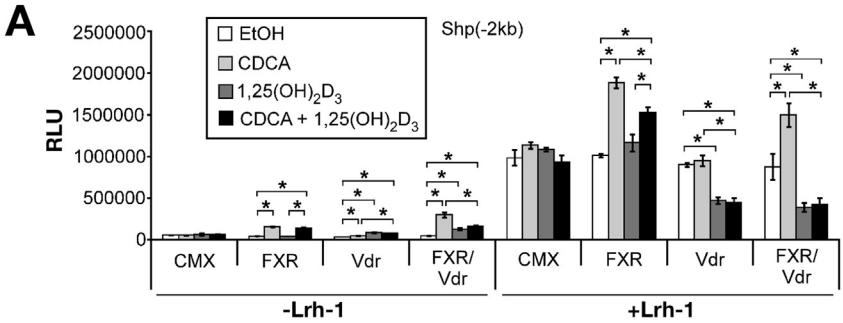
A
Shp(-2kb)
EtOH
CDCA
1,25(OH)2D3
CDCA + 1,25(OH)2D3
RLU
2500000
2000000
1500000
1000000
500000
0
CMX
FXR
Vdr
FXR/ Vdr
-Lrh-1
+Lrh-1

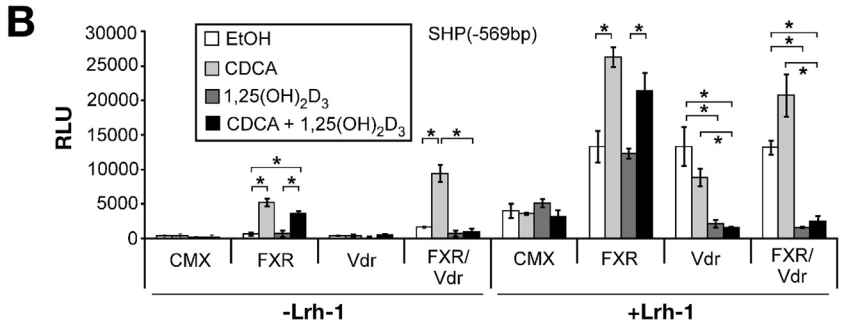
B
SHP(-569bp)
EtOH
CDCA
1,25(OH)2D3
CDCA + 1,25(OH)2D3
RLU
30000
25000
20000
15000
10000
5000
0
CMX
FXR
Vdr
FXR/ Vdr
-Lrh-1
+Lrh-1

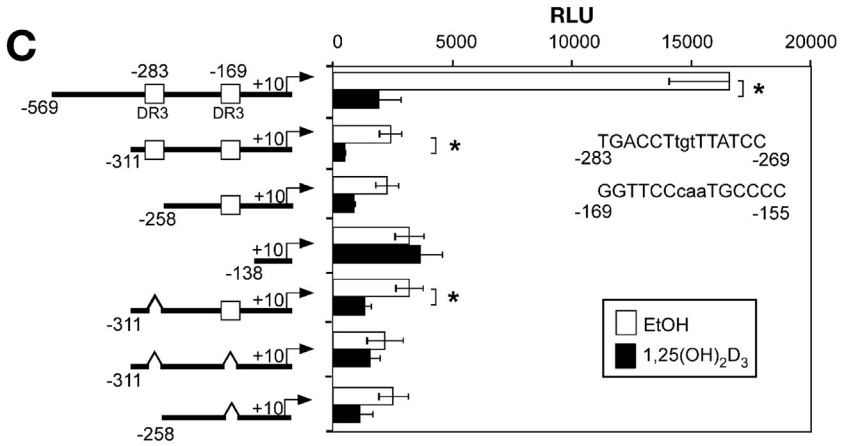
C
RLU
0
5000
10000
15000
20000
-283
-169
+10
-569
DR3
DR3
-311
-258
-138
TGACCTtgtTTATCC
-283
-269
GGTTCCcaaTGCCCC
-169
-155
EtOH
1,25(OH)2D3

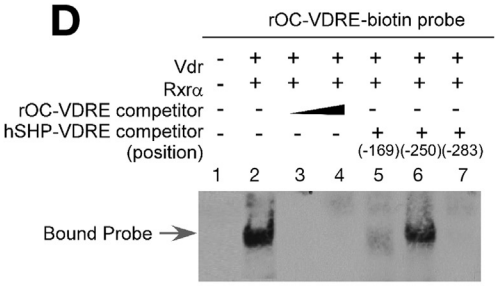
D
rOC-VDRE-biotin probe
Vdr
Rxrα
rOC-VDRE competitor
hSHP-VDRE competitor
(position)
(-169)(-250)(-283)
1 2 3 4 5 6 7
Bound Probe

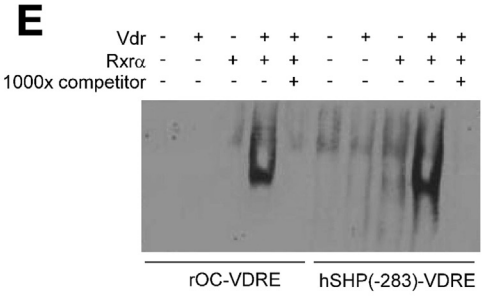
E
Vdr
Rxrα
1000x competitor
rOC-VDRE
hSHP(-283)-VDRE

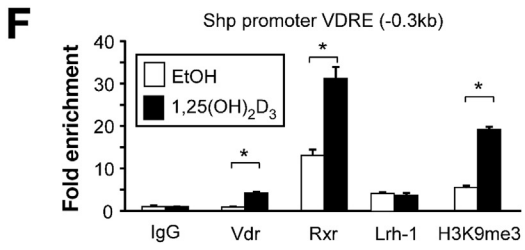
F
Shp promoter VDRE (-0.3kb)
Fold enrichment
40
30
20
10
0
EtOH
1,25(OH)2D3
IgG
Vdr
Rxr
Lrh-1
H3K9me3

$Shp^{-/-}$ (Figure 6*D*) mice, and increased fecal bile acid excretion of tauro-β-muricholic acid and taurocholate in Western-diet–fed wild-type and $Fxr^{-/-}$, but not $Shp^{-/-}$ mice, where a higher bile acid pool size but decreased fecal excretion composed mostly of lithocholic acid and deoxycholic acid were observed (Supplementary Figure 1*C*). Accordingly, plasma and liver cholesterol were reduced in Western-diet–fed $Fxr^{-/-}$ mice with $1,25(OH)_2D_3$ treatment (Figure 6*B*), but not for plasma ($P = .057$) and liver ($P = .23$) cholesterol of Western-diet–fed $Shp^{-/-}$ mice (Figure 6*E*). Hepatic Shp mRNA expression was reduced and ileal Asbt mRNA returned to basal levels in $1,25(OH)_2D_3$-treated, Western-diet–fed $Fxr^{-/-}$ mice (Figure 6*C*), and ileal Fgf15 mRNA was decreased in both Western-diet–fed, $1,25(OH)_2D_3$-treated $Fxr^{-/-}$ and $Shp^{-/-}$ mice (Figures 6*C* and *F*).

Vdr Represses Shp/SHP Promoter Activity

To examine if Vdr suppressed Shp/SHP directly, we performed luciferase reporter assays with proximal Shp/SHP promoters of mouse (−2 kb) and human (−0.5 kb). CDCA significantly increased Shp/SHP promoter activity in the presence of FXR (Figures 7*A* and *B*); in addition, basal Shp/SHP promoter activation was increased with co-transfection of the competence factor, Lrh-1.[2] Addition of $1,25(OH)_2D_3$ and Vdr strongly repressed Shp/SHP promoter activity, and addition of CDCA and $1,25(OH)_2D_3$ led to Vdr-mediated repression of Shp/SHP promoter activities that dominated over FXR-mediated activation, and the observation was independent of Lrh-1 (Figure 7*A* and *B*).

To identify which residues in human SHP promoter conferred repression by Vdr, we generated a number of truncation mutants in the luciferase (luc) reporter and tested for loss of repression after addition of $1,25(OH)_2D_3$ and Vdr (Figure 7*C*). Sequence analysis revealed 2 putative DR3 VDR response elements (VDREs) located within the proximal SHP promoter (at positions −283 and −169; Supplementary Table 2). The ability of $1,25(OH)_2D_3$ to repress the SHP −258-luc reporter was diminished compared with that of −311-luc reporter, and abolished in the −138-luc reporter, consistent with the idea that these 2 predicted VDREs are contributing to the repression by $1,25(OH)_2D_3$. Deletion analysis confirmed involvement of the −283 and −169 VDREs in the $1,25(OH)_2D_3$-mediated suppression of the SHP promoter. When the major putative VDREs were tested for their ability to compete with the known interaction of Vdr/Rxrα on the rat osteocalcin gene (rOC-VDRE), excess unlabeled SHP-VDRE (−283) abolished binding of the protein complex, and the SHP-VDRE(−169) only partially competed for Vdr/Rxrα binding to the rOC-VDRE (Figure 7*D*); a third weak putative VDRE (−250) failed to compete with rOC-VDRE binding. These data are consistent with the promoter truncation analyses that indicate multiple binding sites are important for the $1,25(OH)_2D_3$-mediated repression of the SHP promoter.

EMSA

EMSA experiments were conducted with biotinylated SHP (−283) and (−169) oligonucleotides to test whether the Vdr-Rxrα complex was binding directly to these sites. A distinct protein-DNA complex was formed with SHP (−283)-VDRE, consistent with direct binding of Vdr/Rxrα to this site (Figure 7*E*) that was diminished upon addition of unlabeled competitor. No binding was observed for the putative site at −169 (data not shown). Taken together, we propose that the $1,25(OH)_2D_3$-mediated suppression of SHP expression occurs through the direct binding of VDR to at least one DR3 response element in the proximal SHP promoter.

ChIP Assay

To determine whether VDR binds to the mouse Shp promoter in vivo, we performed ChIP with mouse liver samples at 12 hours after the fourth dose of $1,25(OH)_2D_3$ treatment, whereby Cyp7a1 protein was increased (70%; data not shown). A significant increase in the recruitment of Vdr and Rxrα to the Shp promoter was found with $1,25(OH)_2D_3$, without changes in Lrh-1 recruitment (Figure 7*F*). We observed a $1,25(OH)_2D_3$-dependent increase in histone 3 lysine 9 trimethylation (H3K9me3, a marker of chromatin condensation), further supporting an important role for Vdr in mediating Shp repression (Figure 7*F*).

Figure 7. Interaction between Vdr and the SHP promoter. Human embryonic kidney 293 (HEK293) cells were transiently transfected with either (*A*) mouse Shp (−2 kb)-luciferase reporter or (*B*) human SHP (−569 bp)-luciferase reporter in presence or absence of mouse Lrh-1, Vdr, and human FXR and mouse retinoid X receptor α (Rxrα). After 6 to 8 hours, cells were treated with vehicle (0.1% EtOH), 50 μM CDCA, 0.5 nM $1,25(OH)_2D_3$, or 50 μM CDCA + 0.5 nM $1,25(OH)_2D_3$. Data are mean ± SD (n = 3). *$P < .05$, $1,25(OH)_2D_3$ vs vehicle (EtOH) control; CDCA+$1,25(OH)_2D_3$ vs CDCA; CDCA+$1,25(OH)_2D_3$ vs $1,25(OH)_2D_3$. (*C*) In truncation studies of the SHP promoter, the boxes represent potential VDRE sites, and ⌒ denotes the construct with putative VDRE (sequence shown) deleted. HEK293 cells were transiently transfected with the indicated SHP promoter luciferase constructs in presence of Lrh-1, Rxrα, and Vdr, then treated with vehicle or 0.5 nM $1,25(OH)_2D_3$. Data are mean ± SD (n = 3); *$P < .05$ with or without $1,25(OH)_2D_3$ treatment. (*D*) Vdr/Rxrα heterodimers were incubated with 40 nM rOC-VDRE biotin-labeled probe. Where indicated, an unlabeled oligonucleotide competitor (500-fold that of the probe) was added to the reaction mixtures, except for lane 3, where the competitor concentration was a 100-fold that of the probe. (*E*) Vdr and Rxrα nuclear extracts (alone or in combination) were incubated with 40 nM biotin-labeled rOC-VDRE or SHP(-283)-VDRE. Where indicated, the matching unlabeled oligonucleotide competitor (1000-fold of the probe) was added. (*F*) ChIP assay of Vdr, Rxrα, Lrh-1, and H3K9me3 (IgG as control) at the mouse Shp promoter in liver tissues from vehicle- and $1,25(OH)_2D_3$-treated wildtype mice (n = 3–4/treatment). Quantitative polymerase chain reaction (qPCR) was used to quantify the relative abundance of each species at the Shp promoter. A representative dataset of treated and control mice was shown, and the error bar represents SEM of qPCR triplicates. RLU, relative luciferase unit.

Discussion

We observed cholesterol lowering in response to $1,25(OH)_2D_3$ treatment, an effect associated with elevated Cyp7a1 mRNA and protein expression and microsomal activity, with correspondingly larger bile acid pool sizes and/or greater fecal bile acid excretion in hypercholesterolemic wild-type and $Fxr^{-/-}$ mice. We showed that increased Cyp7a1 expression and activity was achieved via Vdr-repression of Shp after steady-state treatment of $1,25(OH)_2D_3$. The inhibition of Shp and induction of Cyp7a1 by Vdr in mouse livers was clearly demonstrated both in vivo and in vitro, and our molecular studies showed that Vdr activation resulted in repression of Shp/SHP promoter activities (Figure 7). Through extensive gene profiling of the ileum and liver of hypercholesterolemic mouse models, we further ruled out the involvement of other transporters, enzymes, or nuclear receptors known to modulate cholesterol or bile acid processing (Supplementary Figures 2 and 3). All data point to the Fxr-independent and Shp-dependent mechanism by which Vdr down-regulates Shp to increase Cyp7a1 in cholesterol lowering.

These findings contrast other reports on the down-regulation of mouse hepatic Cyp7a1 mRNA due to Fgf15 induction after a high dose of $1,25(OH)_2D_3$.[10] Such divergent results could be explained by differences in the dosing regimen. The notion that VDR is inhibitory to CYP7A1 in human hepatocytes was based on the absence of substantiating evidence on CYP7A1 protein/activity or cholesterol measurements, or timed-matched control samples[9]; the observations were explained as genomic effects arising from the interaction between VDR and hepatocyte nuclear factor 4α on the CYP7A1 promoter, or as nongenomic effects via activation of the extracellular signal-regulated kinase pathway,[9,28] although the latter was not reproduced in a different cell line.[29] It can be argued that conclusions based solely on in vitro data are debatable because time-dependent gene stability exists, and acute cell-based studies are expected to be sensitive to differences in treatment times and conditions. Indeed, in our in vitro human hepatocyte studies, we show time-dependent changes in CYP7A1 expression (Figure 4*B*). The involvement of Shp/SHP may have been easily missed because SHP mRNA has a short half-life (<30 minutes) due to rapid proteasomal degradation that is under the control of the extracellular signal-regulated kinase pathway.[30] We suggest that longer-term effects of steady-state doses of $1,25(OH)_2D_3$ observed in our in vivo studies likely represent physiologic responses.

In our molecular studies, we confirmed an interaction between the Shp promoter and Vdr protein in the ChIP assay. The addition of VDR ligand resulted in reduced activity of Shp/SHP promoters (Figure 7), explaining the observed cholesterol lowering in mouse in vivo. Chromatin remodeling at the Shp promoter in response to $1,25(OH)_2D_3$ is consistent with ligand-mediated repression, although the relevant co-repressor proteins involved in this process have yet to be identified. Although our data are consistent with a direct role for VDR in hepatocytes, we cannot rule out that intercellular communication between resident liver cells is also occurring in vivo because VDR is also highly expressed and functional in stellate cells.[31] We acknowledge that additional $1,25(OH)_2D_3$-liganded mechanisms can contribute to lowering plasma and liver cholesterol in vivo. Indeed, $1,25(OH)_2D_3$ treatment of HL-60 macrophages can also reduce cholesterol by inhibiting human 3-hydroxy-3-methylglutaryl-CoA reductase activity and increasing acetylcoenzyme A acetyltransferase (ACAT) activity leading to cholesteryl ester accumulation.[32]

The novel mechanism of up-regulation of CYP7A1 after $1,25(OH)_2D_3$ treatment suggests that the VDR is a new therapeutic target for cholesterol lowering. However, the potential utility of this mechanism to treat hypercholesterolemia is limited due to the dose-limiting hypercalcemia of $1,25(OH)_2D_3$[25] or its precursor, 1α-hydroxyvitamin D_3.[13] Use of dietary vitamin D for cholesterol lowering in humans remains somewhat uncertain because only very low levels of $1,25(OH)_2D_3$ are synthesized after ingestion. By contrast, it is not unlikely that vitamin D deficiency would affect cholesterol status.[11] The interplay between the VDR and cholesterol homeostasis in humans requires continued investigation with nonhypercalcemic VDR ligands.

Supplementary Material

Note: To access the supplementary material accompanying this article, visit the online version of *Gastroenterology* at www.gastrojournal.org, and at http://dx.doi.org/10.1053/j.gastro.2013.12.027.

References

1. Chiang JY. Regulation of bile acid synthesis: pathways, nuclear receptors, and mechanisms. J Hepatol 2004; 40:539–551.
2. Lu TT, Makishima M, Repa JJ, et al. Molecular basis for feedback regulation of bile acid synthesis by nuclear receptors. Mol Cell 2000;6:507–515.
3. Zöllner G, Marschall HU, Wagner M, et al. Role of nuclear receptors in the adaptive response to bile acids and cholestasis: pathogenetic and therapeutic considerations. Mol Pharm 2006;3:231–251.
4. Inagaki T, Choi M, Moschetta A, et al. Fibroblast growth factor 15 functions as an enterohepatic signal to regulate bile acid homeostasis. Cell Metab 2005;2:217–225.
5. Makishima M, Lu TT, Xie W, et al. Vitamin D receptor as an intestinal bile acid sensor. Science 2002;296:1313–1316.
6. Wagner M, Zöllner G, Trauner M. Nuclear receptor regulation of the adaptive response of bile acid transporters in cholestasis. Semin Liver Dis 2010;30:160–177.
7. Honjo Y, Sasaki S, Kobayashi Y, et al. 1,25-Dihydroxyvitamin D_3 and its receptor inhibit the chenodeoxycholic acid-dependent transactivation by farnesoid X receptor. J Endocrinol 2006;188:635–643.
8. Jiang W, Miyamoto T, Kakizawa T, et al. Inhibition of LXRα signaling by vitamin D receptor: possible role of VDR in bile acid synthesis. Biochem Biophys Res Commun 2006;351:176–184.

9. Han S, Chiang JY. Mechanism of vitamin D receptor inhibition of cholesterol 7α-hydroxylase gene transcription in human hepatocytes. Drug Metab Dispos 2009;37:469–478.
10. Schmidt DR, Holmstrom SR, Fon Tacer K, et al. Regulation of bile acid synthesis by fat-soluble vitamins A and D. J Biol Chem 2010;285:14486–14494.
11. Wang JH, Keisala T, Solakivi T, et al. Serum cholesterol and expression of ApoAI, LXRβ and SREBP2 in vitamin D receptor knock-out mice. J Steroid Biochem Mol Biol 2009;113:222–226.
12. Nishida S, Ozeki J, Makishima M. Modulation of bile acid metabolism by 1α-hydroxyvitamin D_3 administration in mice. Drug Metab Dispos 2009;37:2037–2044.
13. Ogura M, Nishida S, Ishizawa M, et al. Vitamin D_3 modulates the expression of bile acid regulatory genes and represses inflammation in bile duct-ligated mice. J Pharmacol Exp Ther 2009;328:564–570.
14. **Wang XX, Jiang T**, Shen Y, et al. Vitamin D receptor agonist doxercalciferol modulates dietary fat-induced renal disease and renal lipid metabolism. Am J Physiol Renal Physiol 2011;300:F801–F810.
15. Chow EC, Maeng HJ, Liu S, et al. 1α,25-Dihydroxyvitamin D_3 triggered vitamin D receptor and farnesoid X receptor-like effects in rat intestine and liver in vivo. Biopharm Drug Dispos 2009;30:457–475.
16. Gascon-Barré M, Demers C, Mirshahi A, et al. The normal liver harbors the vitamin D nuclear receptor in nonparenchymal and biliary epithelial cells. Hepatology 2003;37:1034–1042.
17. Ponda MP, Dowd K, Finkielstein D, et al. The short-term effects of vitamin D repletion on cholesterol: a randomized, placebo-controlled trial. Arterioscler Thromb Vasc Biol 2012;32:2510–2515.
18. **Zittermann A, Frisch S**, Berthold HK, et al. Vitamin D supplementation enhances the beneficial effects of weight loss on cardiovascular disease risk markers. Am J Clin Nutr 2009;89:1321–1327.
19. Salehpour A, Shidfar F, Hosseinpanah F, et al. Vitamin D_3 and the risk of CVD in overweight and obese women: a randomised controlled trial. Br J Nutr 2012:1–8.
20. Rahimi-Ardabili H, Pourghassem Gargari B, Farzadi L. Effects of vitamin D on cardiovascular disease risk factors in polycystic ovary syndrome women with vitamin D deficiency. J Endocrinol Invest 2013;26:28–32.
21. **Karhapää P, Pihlajamäki J**, Pörsti I, et al. Diverse associations of 25-hydroxyvitamin D and 1,25-dihydroxyvitamin D with dyslipidaemias. J Intern Med 2010;268:604–610.
22. Schwartz JB. Effects of vitamin D supplementation in atorvastatin-treated patients: a new drug interaction with an unexpected consequence. Clin Pharmacol Ther 2009;85:198–203.
23. Davis W, Rockway S, Kwasny M. Effect of a combined therapeutic approach of intensive lipid management, omega-3 fatty acid supplementation, and increased serum 25 (OH) vitamin D on coronary calcium scores in asymptomatic adults. Am J Ther 2009;16:326–332.
24. Chow EC, Durk MR, Cummins CL, et al. 1α,25-Dihydroxyvitamin D_3 up-regulates P-glycoprotein via the vitamin D receptor and not farnesoid X receptor in both *fxr(-/-)* and *fxr(+/+)* mice and increased renal and brain efflux of digoxin in mice *in vivo*. J Pharmacol Exp Ther 2011;337:846–859.
25. Chow EC, Quach HP, Vieth R, et al. Temporal changes in tissue 1α,25-dihydroxyvitamin D_3, vitamin D receptor target genes, and calcium and PTH Levels after 1,25$(OH)_2D_3$ treatment in mice. Am J Physiol Endocrinol Metab 2013;304:E977–E989.
26. **Patel R, Patel M**, Tsai R, et al. LXRβ is required for glucocorticoid-induced hyperglycemia and hepatosteatosis in mice. J Clin Invest 2011;121:431–441.
27. Zierold C, Mings JA, DeLuca HF. Regulation of 25-hydroxyvitamin D_3-24-hydroxylase mRNA by 1,25-dihydroxyvitamin D_3 and parathyroid hormone. J Cell Biochem 2003;88:234–237.
28. Han S, Li T, Ellis E, et al. A novel bile acid-activated vitamin D receptor signaling in human hepatocytes. Mol Endocrinol 2010;24:1151–1164.
29. Wu FS, Zheng SS, Wu LJ, et al. Calcitriol inhibits the growth of MHCC97 heptocellular cell lines by down-modulating c-met and ERK expressions. Liver Int 2007;27:700–707.
30. Miao J, Xiao Z, Kanamaluru D, et al. Bile acid signaling pathways increase stability of small heterodimer partner (SHP) by inhibiting ubiquitin-proteasomal degradation. Genes Dev 2009;23:986–996.
31. Ding N, Yu RT, Subramaniam N, et al. A vitamin D receptor/SMAD genomic circuit gates hepatic fibrotic response. Cell 2013;153:601–613.
32. Jouni ZE, Winzerling JJ, McNamara DJ. 1,25-Dihydroxyvitamin D_3-induced HL-60 macrophages: regulation of cholesterol and LDL metabolism. Atherosclerosis 1995;117:125–138.

Author names in bold designate shared co-first authorship.

Received December 4, 2012. Accepted December 17, 2013.

Reprint requests
Address requests for reprints to: K. Sandy Pang, PhD, Leslie Dan Faculty of Pharmacy, University of Toronto, 144 College Street, Toronto, Ontario, Canada M5S 3M2. e-mail: ks.pang@utoronto.ca; fax: 416-978-8511.

Acknowledgments
The authors thank Drs Nan Wu and Martin Wagner, Baylor College of Medicine, Texas Medical Center, Houston, for assistance with studies on the bile acid pool sizes of *Shp*$^{-/-}$ mice.

Han-Joo Maeng's current affiliation is College of Pharmacy, Inje University, 607 Obang-dong, Gimhae, Gyeongnam 621-749, South Korea.

Sayeepriyadarshini Anakk's current affiliation is Department of Molecular and Integrative Physiology, University of Illinois, Urbana-Champaign, Urbana, IL.

Conflicts of interest
The authors disclose no conflicts.

Funding
The authors (KSP, CC, ECYC, LM, HPQ, and MRD) gratefully acknowledge support from the Canadian Institutes of Health Research, the Natural Sciences and Engineering Research Council of Canada, and the Ontario Graduate Scholarship Program. SA and DDM were supported by CPRIT grant RP120138, and R. P. Doherty, Jr. – Welch Chair in Science Q-0022.

Supplementary Methods

Materials

The $1,25(OH)_2D_3$ was purchased from Sigma-Aldrich Canada (Mississauga, ON). Antibodies against Cyp7a1/CYP7A1 (N-17) were from Santa Cruz Biotechnology (Santa Cruz, CA); those for Gapdh/GAPDH (6C5), Lamin B1, and VDR (9A7) were from Abcam (Cambridge, MA). For the ChIP studies, the following antibodies were used: 10 μg of VDR (sc-13133x, Santa-Cruz Biotechnology), 10 μg of RXR (sc- 774x, Santa-Cruz Biotechnology), 10 μg of LRH-1 (H2325, R&D Systems) or 2 μg of H3K9me3 (ab8898, Abcam) antibodies overnight and used for immunoprecipitation. Male C57BL/6 mice were obtained from Charles River (Senneville, Quebec, Canada) and *Fxr*$^{-/-}$ mice (C57BL/6 background) were kind gifts from Dr Frank J. Gonzalez (National Institutes of Health, Bethesda, MD). The *Shp*$^{-/-}$ mice (C57BL/6 background), aged 8 to 12 weeks, were from the laboratory of Dr David M. Moore (Baylor College of Medicine, Houston, TX). Studies were performed in accordance with institutionally approved animal protocols.

Plasmids

The pCMX, pCMX-hRXRα, pCMX-mRXRα, pCMX-mLRH-1, pGEM, pCMX-β-galactosidase, hSHP(569)-luc, and hSHP (371)-luc were from Dr David Manglesdorf (University of Texas Southwestern Medical Center, Dallas, TX), pEF-mVDR was from Dr Rommel G. Tirona (University of Western Ontario, London, ON), and mSHP promoter was from Dr Li Wang (University of Utah, UT). Human SHP promoter deletion constructs were generated by polymerase chain reaction (PCR) amplification. The PCR fragments were ligated into the *HindIII* and *BglII* sites of the luciferase reporter pGL3 (Promega, Madison, WI) to generate hSHP(238)-luc and hSHP(138)-luc.

Real-Time PCR

Primer sequences are described in Supplementary Methods Table 1. Total mRNA extraction and quantitative PCR procedures are previously described.[1] mRNA levels are normalized to cyclophilin (for mouse liver and hepatocytes), GAPDH (for human hepatocytes), or villin (mouse intestine) then expressed as relative mRNA expression of the control.

Western Blotting

Vdr and Cyp7a1/CYP7A1 protein expression was determined by Western blotting methods, as described,[1,2] after loading of 50 μg total protein samples onto 10% sodium dodecyl sulfate-polyacrylamide gels and transferring to nitrocellulose membranes.[1]

Liver nuclear protein, microsomes, and Cyp7a1 activity. Liver nuclear protein and microsomes for Western blotting were described.[1] For activity assays, mouse liver microsomes (2 mg) obtained from sequential centrifugation were incubated with cholesterol and a reduced nicotinamide adenine dinucleotide phosphate (NADPH) generating system to determine the Cyp7a1 activity according to the high-performance liquid chromatography assay.[1]

Bile acid pool size in hypercholesterolemic mice. Wild-type, Fxr$^{-/-}$ and Shp$^{-/-}$ mice fed the Western diet for 3 weeks were treated with either vehicle or $1,25(OH)_2D_3$ (2.5 μg/kg, every other day for 8 days) at the beginning of the third week (each mouse was caged individually). The extraction procedure for bile acid pool was similar to those described by others.[3,4] On the last day of the study, mice were fasted for 4 hours before induction of anesthesia. The intact gall bladder, liver, and intestine were removed altogether. The tissues were reduced to fine pieces and placed in a beaker containing 50 mL anhydrous ethanol. After the addition of 50 μL of the internal standard (1 mg/mL chenodeoxycholic acid-D_4 [CDCA-d_4] in methanol, C/D/N Isotopes; Pointe-Claire, Quebec, Canada), the content was boiled at 80°C for 1 hour. After cooling, the extracts were filtered through a Whatman filter paper and brought up to 50 mL in a volumetric flask with anhydrous ethanol. Then 500 μL of the extract was centrifuged and filtered through an Ultra-free-MC centrifugal filter device containing 0.22-μm polyvinylidene difluoride membrane (Millipore, Billerica, MA) before analysis. Standard solutions containing known amounts of bile acids were processed and extracted in the same manner. Samples were then analyzed by liquid chromatography-tandem mass spectrometry using 6410 Triple Quad LC/MS instrument (Agilent Technologies) with Electrospray ionization (ESI) source in negative ion mode as described previously, with slight modifications.[5] Samples (1 μL) were separated on a Zorbax XDB-C18 column (4.6 $\times$ 50 mm, 3.5 μm) with a C18 guard column at 0.4 mL/min. The mobile phase consisted of high-performance liquid chromatography−grade water/10 mM NH_4Ac/0.024% formic acid (Solvent A) and methanol/0.024% formic acid (Solvent B). A gradient was utilized over 30 minutes: 0−15 minutes, 70%−80% (Solvent B); 15−17 minutes, 80% (Solvent B); 17−20 minutes, 80%−95% (Solvent B); 20−26 minutes, 95% (Solvent B). Mass spectrometry parameters were as follows: gas temperature 350°C, nebulizer pressure 35 psi, drying gas (nitrogen) 12 L/min, VCap 6000 V (negative), and column temperature 40°C. The fragmentor voltage was 200 V and collision energy was 5 V for all the compounds monitored. Selective ion monitoring was used to detect the conjugated and unconjugated bile acids (Supplementary Methods Table 2). Bile acids were quantified based on peak areas using external calibration curves of standards prepared in methanol. CDCA-d_4 was used to calculate the recovery of bile acids after extraction relative to a blank control.

Plasma and tissue cholesterol. Total plasma cholesterol was determined by the Total Cholesterol Kit (Wako Diagnostics, Richmond, VA). For liver cholesterol measurements, lipids were extracted from approximately 0.2 g liver, homogenized in chloroform:methanol (2:1, v/v),

as described previously,[6] and cholesterol concentrations were determined from extracts using Infinity Cholesterol reagents (Thermo Scientific, Rockford, IL).

Determination of tissue 1α,25-dihydroxyvitamin D_3. The $1,25(OH)_2D_3$ concentrations in mouse plasma and liver were assayed using an enzyme-immunoassay kit.[7] Briefly, weighed liver samples were added to double-distilled water up to 1 mL. The sample was homogenized with 3.75 mL of a mixture of methylene chloride and methanol (1:2 v/v). Then 1.25 mL of methylene chloride was added, mixed for 1 minute, followed by addition of 1.25 mL double-distilled water and mixed for another minute, before centrifugation at 3000 rpm for 20 minutes at room temperature. The extractant (bottom phase) was retrieved by a glass syringe−metal needle set. The extraction procedure was repeated with another 1.25 mL methylene chloride. The recovered, bottom extractant was pooled with that from the previous extraction, dried under N_2, and reconstituted in 0.3 mL charcoal-stripped human serum and analyzed by the enzyme immunoassay kit (Immunodiagnostics Systems Inc., Scottsdale, AZ).

Human hepatocytes. Fresh, human primary hepatocytes from 3 donors (donor ID# Hu1177, Hu1210, Hu1284) were supplied by Dr Jasminder Sahi (Life Technologies; parent company of Invitrogen) as kind gifts. Human hepatocytes (donor ID# Hu1284, male, Caucasian, age 51 years), which showed a stable and high VDR and CYP7A1 mRNA expression (C_T value approximately 26−27 and approximately 23−24, respectively), were treated with $1,25(OH)_2D_3$ and were harvested at various time points to examine changes in mRNA and protein expression.

Supplementary References

1. Chow EC, Maeng HJ, Liu S, et al. 1α,25-Dihydroxyvitamin D_3 triggered vitamin D receptor and farnesoid X receptor-like effects in rat intestine and liver *in vivo*. Biopharm Drug Dispos 2009;30:457–475.
2. Chow EC, Durk MR, Cummins CL, et al. 1α,25-Dihydroxyvitamin D_3 up-regulates P-glycoprotein via the vitamin D receptor and not farnesoid X receptor in both *fxr(-/-)* and *fxr(+/+)* mice and increased renal and brain efflux of digoxin in mice *in vivo*. J Pharmacol Exp Ther 2011;337:846–859.
3. Turley SD, Schwarz M, Spady DK, et al. Gender-related differences in bile acid and sterol metabolism in outbred CD-1 mice fed low- and high-cholesterol diets. Hepatology 1998;28:1088–1094.
4. Zhang Y, Breevoort SR, Angdisen J, et al. Liver LXRα expression is crucial for whole body cholesterol homeostasis and reverse cholesterol transport in mice. J Clin Invest 2012;122:1688–1699.
5. Lee YK, Schmidt DR, Cummins CL, et al. Liver receptor homolog-1 regulates bile acid homeostasis but is not essential for feedback regulation of bile acid synthesis. Mol Endocrinol 2008;22:1345–1356.
6. Patel R, Patel M, Tsai R, et al. LXRβ is required for glucocorticoid-induced hyperglycemia and hepatosteatosis in mice. J Clin Invest 2011;121:431–441.
7. Chow EC, Quach HP, Vieth R, et al. Temporal changes in tissue 1α,25-dihydroxyvitamin D_3, vitamin D receptor target genes, and calcium and PTH levels after 1, $25(OH)_2D_3$ treatment in mice. Am J Physiol Endocrinol Metab 2013;304:E977–E989.

Supplementary Table 1. Plasma Calcium, Phosphorus, ALT, and Portal Bile Acid Concentrations in Wild-Type ($Fxr^{+/+}$) and $Fxr^{-/-}$ Mice Fed a Normal Diet (ND) and in Wild-Type, $Fxr^{-/-}$, and $Shp^{-/-}$ Mice Fed a Western Diet (WD)

	Plasma calcium, *mg/dL*	Plasma phosphorus, *mg/dL*	Plasma ALT, *IU/mL*	Portal bile acid concentration, μM
Wild-type				
Vehicle control−ND	9.6 ± 0.2	19.2 ± 0.9	10.2 ± 0.9	28.5 ± 7.1
1,25(OH)$_2$D$_3$ treated−ND	12.5 ± 0.2[a]	18.7 ± 0.7	11.4 ± 1.2	32.4 ± 9.5
$Fxr^{-/-}$				
Vehicle control−ND	8.1 ± 0.4[b]	19.8 ± 1.3	144 ± 19[b]	53.4 ± 6.8
1,25(OH)$_2$D$_3$ treated−ND	10.0 ± 0.6[a]	17.3 ± 0.8	32.4 ± 4.7[a]	65.0 ± 11.1
Wild-type				
Vehicle control−ND	9.1 ± 0.1	17.3 ± 0.9	7.2 ± 1.6	33.8 ± 14.9
Vehicle control−WD	9.0 ± 0.1	21.1 ± 1.0[c]	23.5 ± 2.3[c]	31.8 ± 6.6
1,25(OH)$_2$D$_3$ treated−WD	12.8 ± 0.5[d]	19.5 ± 0.6	17.2 ± 2.7	31.0 ± 2.6
$Fxr^{-/-}$				
Vehicle control−ND	8.1 ± 0.4	19.8 ± 1.3	96.3 ± 9.0	27.6 ± 6.5
Vehicle control−WD	11.4 ± 0.44[c]	20.9 ± 0.75	81.4 ± 59.9	62.7 ± 10.0[c]
1,25(OH)$_2$D$_3$ treated−WD	17.1 ± 0.59[d]	21.6 ± 0.86	89.2 ± 54.3	80.1 ± 25.5
$Shp^{-/-}$				
Vehicle control−ND	9.3 ± 0.2	15.8 ± 1.1	12.0 ± 2.0	28.3 ± 9.0
Vehicle control−WD	11.0 ± 0.6[c]	24.3 ± 2.2[c]	23.7 ± 4.5	56.0 ± 10.7
1,25(OH)$_2$D$_3$ treated−WD	13.7 ± 0.4[d]	16.2 ± 1.4[d]	46.2 ± 14.7	101 ± 37.3

NOTE. Plasma was diluted 350-fold with 1% HNO_3 and calcium and phosphorus were determined by inductively coupled plasma atomic emission spectroscopy. Plasma ALT and serum portal bile acid concentrations were determined by ALT kit (Bioquant, Nashville, TN) and the total bile acids assay kit (Diazyme, Poway, CA), respectively. Mice fed a normal diet (ND) showed approximately 23% to 30% increase in calcium when treated with 1,25(OH)$_2$D$_3$. The same was observed in Western Diet (WD)-fed $Fxr^{-/-}$ and $Shp^{-/-}$ mice vs their untreated WD-fed counterparts. There was no dramatic change in plasma phosphorous and ALT levels, and total serum bile acid (portal) concentration with 1,25(OH)$_2$D$_3$ treatment. Data represented mean ± SEM (n = 4−8).

ALT, alanine aminotransferase.

[a] $P < .05$, compared with vehicle control (Mann-Whitney *U* test).

[b] $P < .05$, compared with $Fxr^{+/+}$ control (Mann-Whitney *U* test).

[c] $P < .05$, compared with normal diet vehicle control (Mann-Whitney *U* test).

[d] $P < .05$, compared with Western diet vehicle control (Mann-Whitney *U* test).

Supplementary Table 2. Oligonucleotide Sequences for EMSA

Oligonucleotide	5′ → 3′
rOC-VDRE(+)	GCACTGGGTGAATGAGGACATTAC
hSHP(−283)-VDRE(+)	GTTAATGACCTTGTTTATCCACTTG
hSHP(−250)-VDRE(−)	GATAAGGGGCAGCTGAGTGAGCGGC
hSHP(−169)-VDRE(+)	CGTGGGGTTCCCAATGCCCCCTCCC

H, human.

Supplementary Methods Table 1. Mouse and Human Primer Sequences for Quantitative Polymerase Chain Reaction

	Gene bank no.	Forward (5′ → 3′ sequence)	Reverse (5′ → 3′ sequence)
mVdr	NM_009504	GAGGTGTCTGAAGCCTGGAG	ACCTGCTTTCCTGGGTAGGT
mFxr	NM_009108	CGGAACAGAAACCTTGTTTCG	TTGCCACATAAATATTCATTGAGATT
mShp	NM_011850	CAGCGCTGCCTGGAGTCT	AGGATCGTGCCCTTCAGGTA
mLrh-1	NM_001159769	CCCTGCTGGACTACACGGTTT	CGGGTAGCCGAAGAAGTAGCT
mLxrα	NM_013839	GGATAGGGTTGGAGTCAGCA	GGAGCGCCTGTTACACTGTT
mHnf-4α	NM_008261	CCAAGAGGTCCATGGTGTTTAAG	GTGCCGAGGGACGATGTAGT
mFgf15	NM_008003	ACGGGCTGATTCGCTACTC	TGTAGCCTAAACAGTCCATTTCCT
mIbabp	NM_008375.1	CAAGGCTACCGTGAAGATGGA	CCCACGACCTCCGAAGTCT
mApoE	NM_009696.3	AAGCAACCAACCCTGGGAG	TGCACCCAGCGCAGGTA
mVldlr	NM_001161420.1	GAGCCCCTGAAGGAATGCC	CCTATAACTAGGTCTTTGCAGATATGG
mLdlr	NM_010700.2	AGGCTGTGGGCTCCATAGG	TGCGGTCCAGGGTCATCT
mSr-b1	NM_016741.1	GGGAGCGTGGACCCTATGT	CGTTGTCATTGAAGGTGATGT
mCyp7a1	NM_007824	AGCAACTAAACAACCTGCCAGTACTA	GTCCGGATATTCAAGGATGCA
mCyp8b1	NM_010012.3	GCCTTCAAGTATGATCGGTTCCT	GATCTTCTTGCCCGACTTGTAGA
mCyp24a1	NM_009996	CTGCCCCATTGACAAAAGGC	CTCACCGTCGGTCATCAGC
mCyp27a1	NM_024264.4	CTGCGTCAGGCTTTGAAACA	TCGTTTAAGGCATCCGTGTAGA
mHMG CoA Reductase	NM_008255.2	CAAGGAGCATGCAAAGACAA	GCCATCACAGTGCCACATAC
mNpc1l1	NM_207242.2	TGGACTGGAAGGACCATTTCC	GCGCCCCGTAGTCAGCTAT
mAbca1	NM_013454.3	CGTTTCCGGGAAGTGTCCTA	CTAGAGATGACAAGGAGGATGGA
mAbcg5	NM_031884.1	TCAATGAGTTTTACGGCCTGAA	GCACATCGGGTGATTTAGCA
mAbcg8	NM_026180.2	TGCCCACCTTCCACATGTC	ATGAAGCCGGCAGTAAGGTAGA
mBsep	NM_021022.3	ACAGCACTACAGCTCATTCAGAG	TCCATGCTCAAAGCCAATGATCA
mAsbt	NM_011388	GATAGATGGCGACATGGACCTC	CAATCGTTCCCGAGTCAACC
mNtcp	NM_011387.2	ATCTGACCAGCATTGAGGCTC	CCGTCGTAGATTCCTTGCTGT
mOstα	NM_145932.3	TACAAGAACACCCTTTGCCC	CGAGGAATCCAGAGACCAAA
mOstβ	NM_178933.2	GTATTTTCGTGCAGAAGATGCG	TTTCTGTTTGCCAGGATGCTC
mVillin	NM_009509	TCCTGGCTATCCACAAGACC	CTCTCGTTGCCTTGAACCTC
mCyclophillin	X58990	GGAGATGGCACAGGAGGAA	GCCCGTAGTGCTTCAGCTT
hCYP7A1	NM_000780.3	GAATGCTGGTCAAAAAGTC	TGAAATCCTCCTTAGCTGT
hCYP24A1	NM_000782	CAGCGAACTGAACAAATGGTCG	TCTCTTCTCATACAACACGAGGCAG
hGAPDH	NM_002046	GAAGGTGAAGGTCGGAGTC	GAAGATGGTGATGGGATTTC

h, human; m, mouse.

Supplementary Methods Table 2. Summary of Liquid Chromatography-Tandem Mass Spectrometry Parameters Used to Quantify Bile Acids

Compound	Retention time, *min*	Ion monitored $[M\text{-}H]^-$, *m/z*
Taurocholic acid: tCA	10.4	514→514
Cholic acid: CA	21.2	407→407
Deoxycholic acid: DCA/Chenodeoxycholic acid: CDCA	23.7	391→391
Tauro-β-muricholic acid: tβ-MCA	4.3	514→514
Lithocholic acid: LCA	24.3	375→375
Chenodeoxycholic acid-d4: CDCA-d4	23.2	395→395

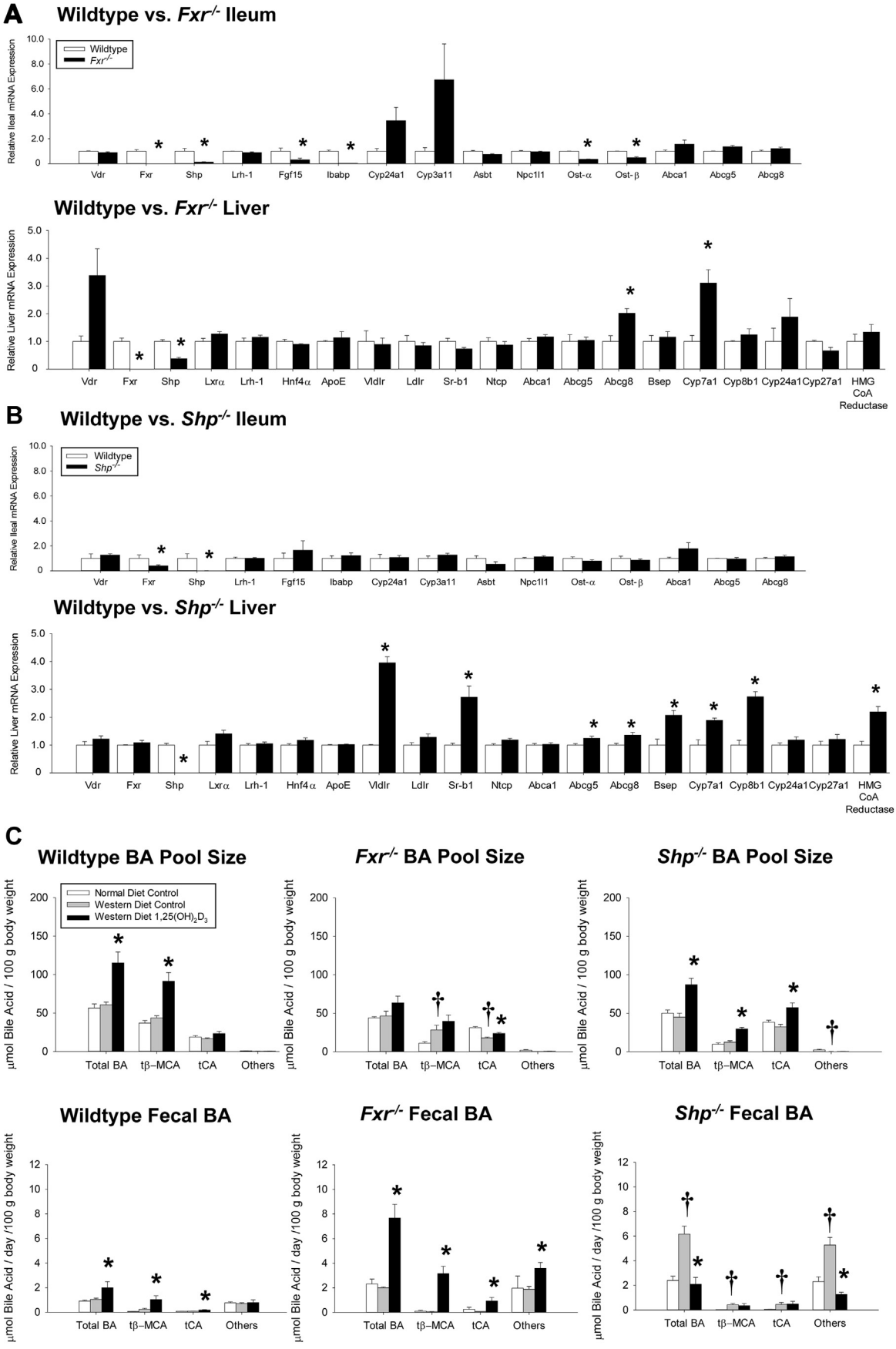
A
Wildtype vs. Fxr-/- Ileum
Wildtype
Fxr-/-
Relative Ileal mRNA Expression
Vdr Fxr Shp Lrh-1 Fgf15 Ibabp Cyp24a1 Cyp3a11 Asbt Npc1l1 Ost-α Ost-β Abca1 Abcg5 Abcg8
Wildtype vs. Fxr-/- Liver
Relative Liver mRNA Expression
Vdr Fxr Shp Lxrα Lrh-1 Hnf4α ApoE Vldlr Ldlr Sr-b1 Ntcp Abca1 Abcg5 Abcg8 Bsep Cyp7a1 Cyp8b1 Cyp24a1 Cyp27a1 HMG CoA Reductase
B
Wildtype vs. Shp-/- Ileum
Wildtype
Shp-/-
Relative Ileal mRNA Expression
Vdr Fxr Shp Lrh-1 Fgf15 Ibabp Cyp24a1 Cyp3a11 Asbt Npc1l1 Ost-α Ost-β Abca1 Abcg5 Abcg8
Wildtype vs. Shp-/- Liver
Relative Liver mRNA Expression
Vdr Fxr Shp Lxrα Lrh-1 Hnf4α ApoE Vldlr Ldlr Sr-b1 Ntcp Abca1 Abcg5 Abcg8 Bsep Cyp7a1 Cyp8b1 Cyp24a1 Cyp27a1 HMG CoA Reductase
C
Wildtype BA Pool Size
Fxr-/- BA Pool Size
Shp-/- BA Pool Size
Normal Diet Control
Western Diet Control
Western Diet 1,25(OH)2D3
μmol Bile Acid / 100 g body weight
Total BA tβ–MCA tCA Others
Wildtype Fecal BA
Fxr-/- Fecal BA
Shp-/- Fecal BA
μmol Bile Acid / day /100 g body weight
Total BA tβ–MCA tCA Others

Supplementary Figure 1. $1,25(OH)_2D_3$ treatment differentially alters bile acid pool size and fecal bile acid excretion in wildtype, *Fxr*$^{-/-}$ and *Shp*$^{-/-}$ mice. The intestinal and liver genes that affect bile acid processing were first compared among normal diet (ND)-fed wildtype and knockout mice; relative values for wildtype mice were set as unity (A) Absence of Fxr in *Fxr*$^{-/-}$ mice led to reduced Shp, Fgf15, Ibabp, and Ost-α and Ost-β in ileum and lower Shp but increased Abcg8 and Cyp7a1 mRNA expression in liver compared to those of wildtype mice. (B) Absence of Shp in *Shp*$^{-/-}$ mice led to reduced Fxr in ileum and increased Vldlr, Sr-b1, Abcg5, Abcg8, Cyp7a1, Cyp8b1, and HMG CoA reductase mRNA in liver, as found previously.[1,2] *, $P <$ .05, Mann-Whitney U test: between wildtype and *Fxr*$^{-/-}$, ND-fed mice (C) Individual bile acids were quantified by LC/MS using external calibration curves of pure bile acid standards and CDCA-d_4 as an internal standard. "Others" represents the sum of CDCA, CA, LCA, and DCA. In wildtype mice, the Western diet (WD) did not alter amounts of individual bile acids nor their sum (bile acid pool size), but the total bile acid pool size and fecal excretion of bile acids were increased upon treatment of $1,25(OH)_2D_3$ (when Cyp7a1 was increased). In *Fxr*$^{-/-}$ mice, $1,25(OH)_2D_3$ treatment did not significantly increase the total bile acid pool size, however, the fecal excretion of total bile acids and of tβ-MCA and tCA was disproportionately increased relative to the modest change in pool size. We speculate that *Fxr*$^{-/-}$ mice, despite showing increased Cyp7a1 with $1,25(OH)_2D_3$ treatment, do not reabsorb bile acids as efficiently as wildtype mice. Their lower basal expression of intestinal Ostα-Ostβ (30-40% of wildtype mice) and virtually non-existent Ibabp level (see Supplementary Figures 1A and 3A) may give rise to a net, lower reabsorption/reclamation of bile acids and a disproportionately higher fecal excretion of tβ-MCA and tCA. In $1,25(OH)_2D_3$-treated *Shp*$^{-/-}$ mice, the total bile acid pool size was increased, whereas fecal bile acid excretion was dramatically decreased. The *Shp*$^{-/-}$ mice are distinct because the fecal bile acids excreted after $1,25(OH)_2D_3$ treatment reflect primarily products of bile acid conversion by bacteria in the colon (LCA and DCA), whereas in wildtype and *Fxr*$^{-/-}$ mice, $1,25(OH)_2D_3$ treatment significantly increased the levels of the bile acid tβ-MCA in the feces. The difference in the composition of the fecal bile acids under different treatment conditions suggest that, despite the increased bile acid pool size in response to $1,25(OH)_2D_3$ in the *Shp*$^{-/-}$ mouse, this is unlikely to be due to changes in bile acid metabolizing enzymes. $P <$ .05, Mann-Whitney U tests: †, for WD- vs ND-fed mice of same genotype; *, between vehicle vs $1,25(OH)_2D_3$ treated WD-fed, mice of same genotype.

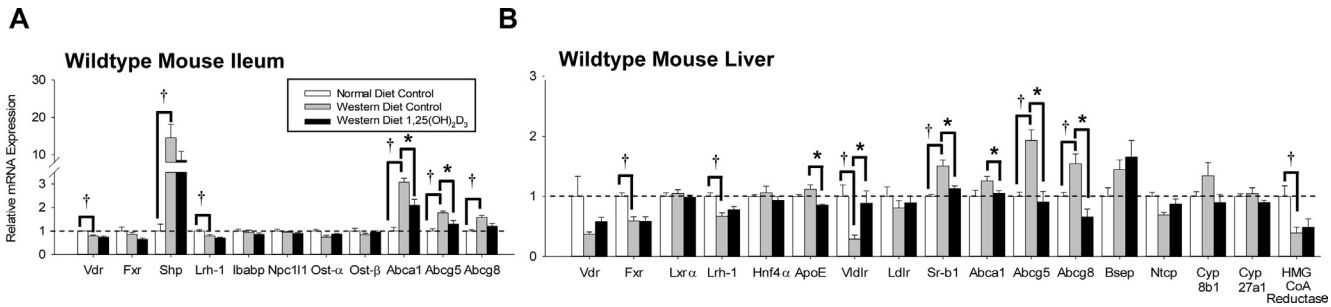

Supplementary Figure 2. Changes in mRNA expression of other cholesterol related genes in (A) ileum and (B) liver of WD-fed wildtype mice treated with 1,25(OH)$_2$D$_3$. A set of vehicle-treated wildtype mice on ND served as controls. (A) Ileal Shp, Abca1, Abcg5, and Abcg8 mRNA expressions were elevated by the WD, and mRNA expression levels of ileal Abca1 and Abcg5 mRNA was decreased upon exposure to 1,25(OH)$_2$D$_3$. (B) Hepatic Sr-b1, Abcg5, and Abcg8 mRNA expressions were increased whereas those for FXR, Vldlr and HMG Co-A reductase were decreased by the WD. Upon 1,25(OH)$_2$D$_3$ treatment, mRNA expression of ApoE, Sr-b1, Abcg5, and Abcg8 were significantly decreased, while Vldlr mRNA was increased back to normal. The symbols † and * denote significant differences ($P < .05$) using Mann-Whitney U test between the ND-fed and WD-fed controls, and between the WD-fed 1,25(OH)$_2$D$_3$-treated vs WD-fed, vehicle-treated control, respectively. Data are the mean ± SEM (n = 4-8).

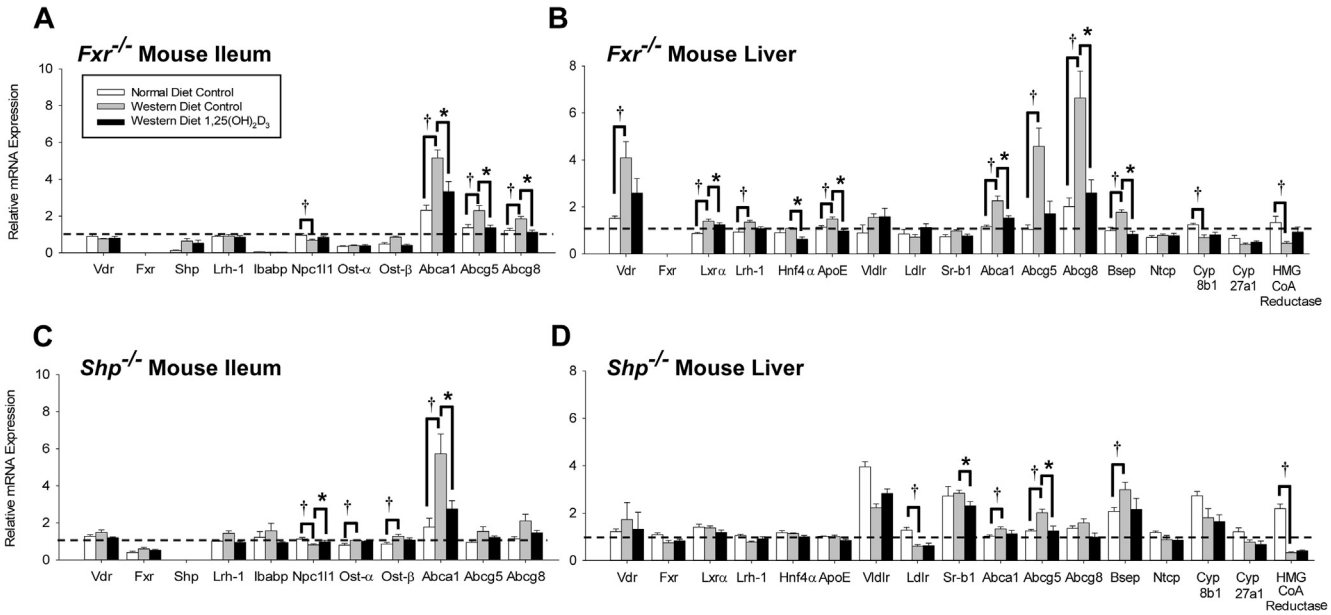

Supplementary Figure 3. Changes in mRNA expression in the (A) ileum (B) livers of WD-fed *Fxr*$^{-/-}$ and *Shp*$^{-/-}$ mice treated with 1,25(OH)$_2$D$_3$; these were compared against the relative abundances for ND-fed wildtype mouse (Supplementary Figure 1) assigned as unity for comparison. In *Fxr*$^{-/-}$ mice, (A) mRNA expression of ileal Abca1, Abcg5, and Abcg8 was elevated by the WD, but returned to basal levels upon treatment of 1,25(OH)$_2$D$_3$, whereas Ileal Npc1l1 mRNA expression was slightly decreased by the WD. (B) mRNA expression levels of hepatic Vdr, Lxrα, Lrh-1, Bsep, ApoE, Abca1, Abcg5, and Abcg8 were all increased by the WD whereas Cyp8b1 and HMG Co-A reductase mRNA levels were decreased; Ntcp was unchanged. Upon 1,25(OH)$_2$D$_3$ treatment, mRNA expression levels of Lxrα, ApoE, Abca1, Abcg8 and Bsep were decreased in WD-fed *Fxr*$^{-/-}$ mice. (C) In *Shp*$^{-/-}$ mice, ileal mRNA expression of Npc1l1 was slightly decreased and that of Abca1 was elevated by the WD. Upon treatment with 1,25(OH)$_2$D$_3$, both ileal Npc1l1 and Abca1 mRNA level returned to basal levels in WD-fed *Shp*$^{-/-}$ mice. (D) In *Shp*$^{-/-}$ mice, hepatic Bsep, Abca1 and Abcg5 mRNA expression was elevated slightly by the WD while Ldlr and HMG Co-A reductase mRNA levels were decreased. Upon 1,25(OH)$_2$D$_3$ treatment, mRNA expression levels of Sr-b1, Abcg5 and Bsep were decreased, but there was no change in HMG CoA reductase, Bsep, or Ntcp. The symbols † and * denote significant differences ($P < .05$) using Mann-Whitney U test between the ND-fed and WD-fed controls, and between the WD-fed 1,25(OH)$_2$D$_3$-treated vs WD-fed, vehicle-treated control, respectively. Data represent the mean ± SEM (n = 4-8).